

# DirPA: Addressing Prior Shift in Imbalanced Few-shot Crop-type Classification

Joana Reuss<sup>a,\*</sup>, Ekaterina Gikalo<sup>a</sup>, Marco Körner<sup>a,b,c</sup>

<sup>a</sup>Technical University of Munich (TUM), TUM School of Engineering and Design, Department of Aerospace and Geodesy, Chair of Remote Sensing Technology, Munich, 80333, Germany

<sup>b</sup>Technical University of Munich (TUM), Munich Data Science Institute (MDSI), Garching, 85748, Germany

<sup>c</sup>ELLIS Unit Jena, University of Jena, Jena, Germany, Jena, 07743, Germany

---

## Abstract

Real-world agricultural monitoring is often hampered by severe class imbalance and high label acquisition costs, resulting in significant data scarcity. In *few-shot learning (FSL)*—a framework specifically designed for data-scarce settings—, training sets are often artificially balanced. However, this creates a disconnect from the long-tailed distributions observed in nature, leading to a distribution shift that undermines the model’s ability to generalize to real-world agricultural tasks. We previously introduced *Dirichlet Prior Augmentation (DirPA; Reuss et al., 2026a)* to proactively mitigate the effects of such label distribution skews during model training. In this work, we extend the original study’s geographical scope. Specifically, we evaluate this extended approach across multiple countries in the *European Union (EU)*, moving beyond localized experiments to test the method’s resilience across diverse agricultural environments. Our results demonstrate the effectiveness of DirPA across different geographical regions. We show that DirPA not only improves system robustness and stabilizes training under extreme long-tailed distributions, regardless of the target region, but also substantially improves individual class-specific performance by proactively simulating priors.

*Keywords:* few-shot learning, DirPA, prior shift, Dirichlet distribution, crop-type classification, EuroCropsML.

---

## 1. Introduction

With climate change on the rise, today’s agricultural practices, as we know them, are severely at risk. Therefore, not only recently, food security has been appointed as one of the 17 *Sustainable Development Goals (SDGs)* of the 2030 Agenda for Sustainable Development by the *United Nations (UN)*. As a result, agriculture-related tasks such as crop mapping, yield estimation, water stress monitoring, and tracking pest or disease outbreaks are becoming increasingly important. The sheer amount of *remote sensing (RS)* data provided by *Earth observation (EO)* and meteorological satellites, as well as the latest advancements in *machine learning (ML)* and, particularly, *deep learning (DL)*, have significantly contributed to solving such tasks, for instance in [Sainte Fare Garnot et al. \(2020\)](#); [Bermúdez et al. \(2017\)](#); [Rußwurm and Körner \(2020\)](#); [Saini and Ghosh \(2018\)](#). However, data-driven DL models require vast amounts of annotated data to achieve acceptable performances. This frequently poses a significant challenge in agricultural applications, as labeled crop data is often rare and unevenly distributed globally, due to high acquisition costs and the impracticality of manual annotation. Consequently, the need for DL approaches that rely less on substantial amounts of data has emerged as a major research direction. A *state-of-the-art (SOTA)* framework that aims to increase model performance on a target task with very limited amounts of data, is *few-shot learning (FSL)*. FSL is typically defined as an  $n$ -way  $k$ -shot problem, where  $n$  defines

the number of distinct classes and  $k$  the number of samples per class. Therefore, in common FSL, the target dataset consists of a balanced training (support) set and a corresponding, also balanced, test (query) set. Conversely, real-world agricultural data is characterized by high class imbalance, with the majority of samples belonging to a limited number of classes (*e.g.*, wheat) and a considerable amount of underrepresented crops (*e.g.*, parsley). Therefore, various studies have recommended the use of arbitrary and imbalanced test sets to better reflect real-world scenarios ([Reuss et al., 2026b](#); [Ochal et al., 2023](#); [Mohammadi et al., 2024](#)). In doing so, we induce a prior distribution shift, where the training prior  $p_{\text{train}}(y)$  differs from the final real-world test prior  $p_{\text{test}}(y)$ , potentially resulting in the model learning a strong, incorrect bias, which often leads to poor generalization ([Reuss et al., 2026b,a](#)).

In the past, such prior shifts have traditionally been addressed, for instance, via the adjustment of class probabilities at inference-time ([Lipton et al., 2018](#); [Kluger et al., 2021](#)), *cf. Section 2*. We previously demonstrated, however, that our novel *Dirichlet Prior Augmentation (DirPA; Reuss et al., 2026a)* method proactively addresses prior shifts during training, leading to improved model performance and robustness without requiring additional inference-time adjustments ([Reuss et al., 2026a](#)). However, while DirPA improved *overall classification accuracy*  $a_{\text{OA}}$  and *Cohen’s kappa*  $\kappa$ , initial experiments showed inferior performance on macro metrics.

Building upon our previous work ([Reuss et al., 2026a](#)), this study represents a major expansion. We now apply DirPA across an extensive geographical area to assess its operational stabil-

---

\* Corresponding author.  
E-Mail address: [joana.reuss@tum.de](mailto:joana.reuss@tum.de) (J. Reuss)

ity and reliability under diverse environmental and agricultural conditions.

The main contributions are:

1. **Geographical expansion:** We apply the DirPA method to a large-scale, real-world dataset covering eight diverse European countries, demonstrating cross-dataset stability.
2. **Imbalance-dependent performance:** We reveal a strong correlation between the dataset’s structural class imbalance and the magnitude of performance gains.
3. **Hierarchical robustness:** We show that DirPA enhances classification reliability by boosting parent-level accuracy and F1-scores, ensuring accurate land-cover identification even when fine-grained distinctions are constrained by data scarcity.

## 2. Related work

We study few-shot crop-type classification under realistic long-tailed label distributions, where balanced training sets induce an artificial prior shift between training and evaluation. In this section, we review the few-shot paradigm, imbalance-aware training frameworks, and prior-shift handling.

### 2.1. Few-shot learning paradigm

A common approach in FSL is to leverage prior knowledge gained from training on a distinct source task. Various approaches have been explored to equip a model with relevant knowledge before being trained on a data-scarce target task, among the most prominent being *transfer learning*, *meta-learning*, and *self-supervised learning (SSL)*. While both meta-learning and SSL have been shown to achieve good performance, they come with high computational costs (Reuss et al., 2026b). Although FSL and the concept of meta-learning are frequently used as synonyms, FSL may also denote a task defined strictly by its low-data constraints (Reuss et al., 2026a). We adopt this broader definition of FSL, acknowledging recent findings on transfer learning—via regular pre-training and subsequent fine-tuning—achieving competitive results compared to complex meta-learning algorithms across a wide range of agricultural applications (Kurian et al., 2024; Alem and Kumar, 2022; Wang et al., 2018; Rouba and Larabi, 2023). Transfer learning leverages the transferability of latent features, assuming that the source-domain knowledge generalizes sufficiently to overcome the lack of samples from the target domain.

#### 2.1.1. Class imbalance

Ochal et al. (2023) provide a detailed comparison and evaluation of various existing few-shot learning methods under class imbalance. They found that classical data-level rebalancing, in particular, random oversampling applied to the support set, yields consistent improvements across different model architectures and imbalance distributions. In contrast, loss-based reweighting strategies, including weighted loss and *focal loss (FL)* (Lin et al., 2020), provide limited or inconsistent gains and generally underperform random oversampling.

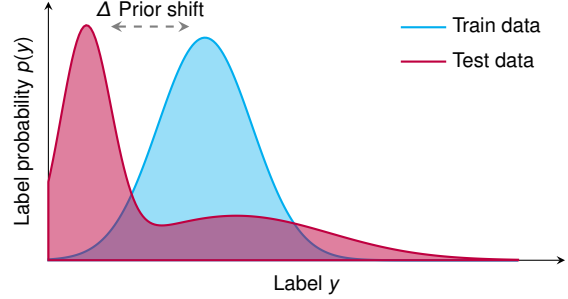


Figure 1. Visualization of a label (prior) distribution shift between train dataset and a long-tailed test dataset.

#### 2.1.2. FSL in remote sensing

In recent years, researchers have widely applied FSL in agricultural applications to address data scarcity. First, Rußwurm et al. (2020) and Wang et al. (2020) demonstrated the superiority of algorithms based on *Model-agnostic Meta-learning (MAML)* (Finn et al., 2017) compared to regular transfer learning on land-cover classification. Tseng et al. (2022) extended the original MAML algorithm to explicitly support agricultural monitoring by incorporating additional metadata, such as spatial coordinates. Furthermore, Keraani et al. (2022) proposed a temporal attention-based encoder for few-shot crop classification and employed transfer learning, training on an imbalanced dataset using FL and data augmentation. Addressing the need for realistic FSL benchmarks, we provided a comprehensive cross-regional benchmark study using the few-shot crop-type dataset EURO-CROPSML (Reuss et al., 2026b, 2025). Their findings show that, while meta-learning achieves superior performances compared to regular transfer learning and self-supervised learning, it comes at the expense of substantially increased computational costs. Moreover, they highlight that none of the evaluated methods were able to overcome the distributional discrepancy between the balanced training set and the imbalanced test set.

#### 2.2. Prior shift in FSL

In FSL, training episodes are typically constructed with balanced class priors, whereas deployment data is often long-tailed. This induces a shift in the label (prior) distribution, as visualized in Figure 1, which biases posterior predictions and can degrade performance. Prior-shift methods, therefore, either estimate the test distribution and recalibrate predictions at inference time or aim to reduce sensitivity to unknown priors during training.

Recent studies often address the problem of prior distribution shifts at inference time. *Black Box Shift Estimation (BBSE)* (Lipton et al., 2018) estimates the test distribution  $p_{\text{test}}(y)$  to improve generalization for symptom-diagnosis detection. Sipka et al. (2022) present a novel prior estimation approach based on confusion matrices, addressing infeasible solutions arising from inconsistent decision probability and confusion matrix estimates.

Kluger et al. (2021) directly tackles the problem of label (prior) and feature (covariate) distribution shift in few-shot crop-type classification using crop statistics, assuming that the distribution of the test set is known. Specifically, to address the prior distribution shift, they reweigh the posterior probabilities.

### 2.3. Dirichlet priors and distribution augmentation

The *Dirichlet distribution*  $\text{Dir}(\alpha)$  is often used to model the prior in Bayesian statistics (Reuss et al., 2026a). Among others, previous work addressed supervised clustering (Daumé III and Marcu, 2005) and the utilization of Dirichlet priors within a Bayesian framework for regression (Rademacher and Doroslov-ački, 2021). The Dirichlet distribution offers several desirable properties as a Bayesian prior (*cf.* Rademacher and Doroslov-ački, 2021). First, it has full support over the space of probability distributions, ensuring that the true data-generating distribution remains learnable regardless of the initial prior specification. Second, it is the conjugate prior for multinomial data (*e.g.*, categorical counts), yielding closed-form posterior distributions that simplify mathematical derivations and improve computational efficiency. Finally, it provides controllable informativeness through the localization parameter  $\alpha_0$ , which explicitly governs the bias-variance trade-off, and allows the prior to range from *highly opinionated* to *effectively non-informative*, depending on the degree of prior knowledge.

Most previous few-shot learning studies employing Dirichlet priors typically assume a balanced training (support) and test (query) set. Consequently, they often use Dirichlet sampling primarily to simulate imbalanced test distributions. Specifically, Veilleux et al. (2021) model the class marginal distribution of the query set as a random variable drawn from a Dirichlet distribution. Their analysis shows that several SOTA transductive few-shot methods implicitly encode a class-balance prior and suffer significant performance degradation under Dirichlet-sampled query sets. Similarly, Mohammadi et al. (2024) adopt Dirichlet-distributed query sampling to evaluate few-shot learning methods for crop mapping. They demonstrate that commonly used balanced-query evaluations systematically overestimate model performance. Using realistic Dirichlet-sampled query sets, they report consistent performance drops across methods. These approaches essentially serve as a few-shot evaluation method, as they solely focus on simulating artificially imbalanced test sets. Contrarily, we introduced Dirichlet priors during training, based on the assumption of having a balanced training set and an imbalanced test set (Reuss et al., 2026a). They employ DirPA, which proactively tackles this distribution shift directly during training by sampling pseudo-priors from the *symmetric* Dirichlet distribution. By learning across a wide variety of priors, the model learns a *prior-agnostic* representation, ensuring stable generalization to real-world imbalanced distributions without requiring prior knowledge of the target domain at test time.

## 3. Dataset

We conduct all training and evaluation on EUROCRPSML 2.0, an extension and refinement of the EUROCRPSML dataset (Reuss et al., 2025). EUROCRPSML provides parcel-level, multi-temporal Sentinel-2 L1C (top-of-atmosphere) observations paired with multi-class crop annotations originating from the EUROCRPS reference dataset (Schneider et al., 2023). All crop labels follow the *Hierarchical Crop and Agriculture Taxonomy (HCAT; Schneider et al., 2023, 2021)*, where, for instance,

Table 1. Dataset details of EUROCRPSML 2.0. The # *Crop classes* column refers to the number of unique crop types in HCAT level 6. The # *Parcels* column refers to unique parcel geometries after removing potential duplicates from the EUROCRPS reference data and filtering out clouds, cirrus, snow, and ice.

Country	# Crop classes	# Parcels
Austria	98	2 589 192
Belgium	136	560 671
Flanders	120	223 269
Wallonia	91	337 402
Estonia	127	175 905
Germany	198	1 632 620
Lower Saxony	150	901 364
North Rhine-Westphalia	175	731 256
Latvia	108	431 143
Lithuania	22	1 101 839
Portugal	84	99 612
Slovakia	121	251 250
Slovenia	112	818 902
Spain	10	962 111
Navarra	10	962 111

level 3 represents general land cover types and level 6 the most-granular crop type, distinguished by seasonality, if applicable.

We extend the geographic coverage of the original EUROCRPSML with 2021 parcel-level crop data from Austria, Belgium (Flanders and Wallonia), Estonia, Germany (*Lower Saxony (LS)* and *North Rhine-Westphalia (NRW)*), Lithuania, Latvia, Portugal, Slovakia, Slovenia, and Spain (Navarra). While we adhere to the original processing pipeline for median-based parcel aggregation, all observations have been reprocessed using the Sentinel-2 L1C Collection 1 (Enache et al., 2023; European Space Agency (ESA), 2021). This ensures a harmonized data standard across the full geographic coverage. Furthermore, we refine the cloud-removal step by also accounting for thin cirrus and snow or ice, following the classification approach of the L2A algorithm (Louis et al., 2022).

### 3.1. Dataset split

We define a universal pre-training dataset comprising Austria and Germany. All other remaining countries are utilized as individual fine-tuning sets. Figure 2 illustrates the pre-training and fine-tuning countries in detail. Pre-training on a joint Austrian-German dataset offers several advantages and specific characteristics, which we outline below.

*Class distribution.* Both countries exhibit diverse class distributions and highly diverse reporting structures, resulting in very fine-grained crop classes. This enables the training of a rich feature extractor and is necessary for a successful transfer to fine-grained target tasks. Specifically, Austria contains 2 589 192 samples, while LS and NRW comprise 901 364 and 731 256 samples, respectively. Despite the larger total sample count in Austria, Germany exhibits a higher number of unique crop classes with very few samples, as shown in Figure 3. Across

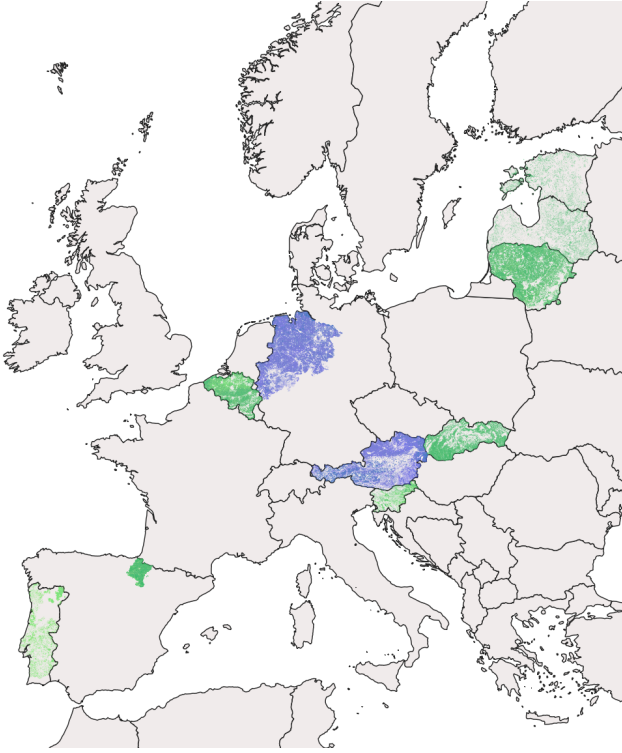


Figure 2. Pre-training and fine-tuning country split. Countries colored in **blue** are used for pre-training, whereas those colored in **green** are used for fine-tuning. The darker the coloring, the denser the labeled agricultural fields.

both Austria and Germany, the *pasture meadow grassland grass* class dominates by a wide margin, accounting for 42% of samples in Germany (LS: 41%, NRW: 43%) and 51% in Austria. When excluding the dominant *pasture meadow grassland grass* class, crop distributions in Germany are similar across LS and NRW. In LS, *grain maize corn popcorn* is the most frequent crop class at 22%, followed by *winter common soft wheat* at 14%. In NRW, *grain maize corn popcorn* contributes 18%, while *winter common soft wheat* accounts for 16%. In contrast, Austria exhibits a different composition, with the most prevalent classes being *tree wood forest* (13%) and *vineyards wine vine rebland grapes* (13%). A detailed visualization of overlapping classes between the pre-training countries and each fine-tuning country is shown in Figure 4. With regard to Spain, the class *not known or other* class is excluded, given its inclusion of all elements not categorized as agricultural fields.

**Biogeographical regions.** Both countries are located in central Europe. Hence, they are mostly characterized by the *Continental* biogeographical zone, with marginal overlaps from the *Alpine* or *Atlantic* regions (European Environment Agency (EEA), 2016), cf. Figure 5. This establishes a *central European baseline* that avoids severe climatic conditions and permits the investigation of varying levels of domain shift.

**Agricultural practices.** Austria is characterized by a higher number of small-scale agricultural fields, with a median field area of 0.46 ha compared to a mean of 1.22 ha. In contrast, NRW and LS exhibit larger typical field sizes, with medians of 1.18 ha

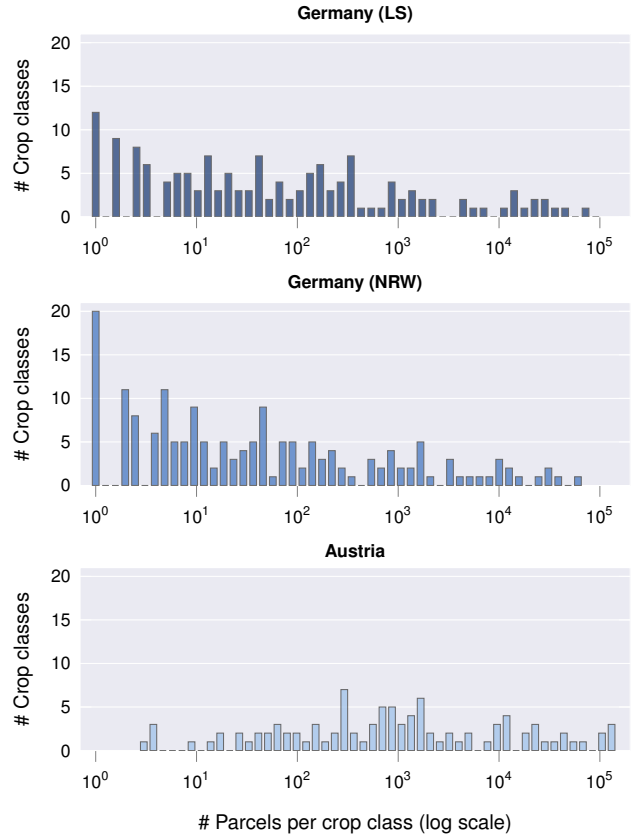


Figure 3. EuroCropsML 2.0 binned class distribution for Germany (LS and NRW) and Austria, shown on a logarithmic scale, with the *pasture meadow grassland grass* class removed.

and 1.86 ha and means of 2.04 ha and 2.87 ha, respectively. As a result, the per-field median-pixel estimates of EUROCropsML 2.0 in Austria are derived from a much smaller number of pixels, thereby increasing their sensitivity to outliers. Conversely, the larger parcel sizes observed in Germany allow for aggregation over a much greater number of pixels, thereby yielding more robust spectral reflectance values.

### 3.2. Fine-tuning split

Most fine-tuning countries exhibit a long-tailed data distribution. Therefore, simply applying a random train, validation, and test split would result in zero-shot classification and non-representative validation sets. Our objective is to establish a robust and realistic training-validation environment while reserving a large, representative set for the final evaluation. Consequently, the overall split was prioritized as follows:

**Test set** 20% of the total dataset for the final, unbiased performance evaluation.

**Validation set** A small, efficient set of 5000 samples for hyperparameter tuning and early stopping.

**Training set** The remaining samples for training.

We employ a class-aware splitting strategy to ensure that all fine-tuning classes are represented in the training set, serving

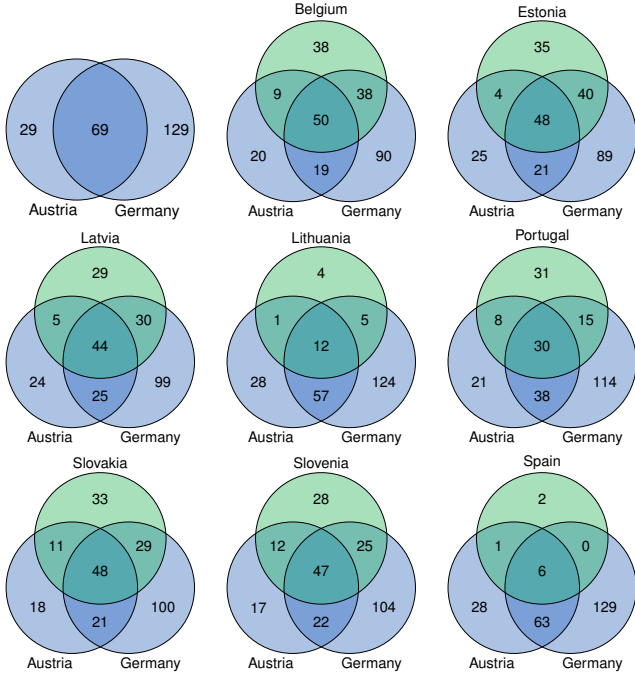


Figure 4. The number of annotated crop classes that are shared and distinct between the pre-training countries—Austria and Germany—and the respective fine-tuning country.

as a prerequisite for assuming known crop types in real-world scenarios. Let  $N_c$  be the total number of available samples for class  $c$ . We employ the following allocation protocol:

1.  $N_c = 1$ : The sample is allocated to the training set.
2.  $N_c = 2$ : One sample is allocated to the training and one to either validation or test.
3.  $N_c = 3$ : One sample is assigned to each subset.
4.  $N_c > 3$ : The samples are randomly distributed between the test and validation sets to fulfill the remaining capacity required to meet the 20% test target and 5000 validation target<sup>1</sup>, while maintaining the class distribution of the original pool. All samples not selected for the validation or test sets are added to the training set.

This strategy ensures that the final validation set, although small, contains a proportional representation of all classes with  $N_c \geq 3$ , thereby preventing evaluation biases. Table 2 gives an overview of the final number of distinct crop classes in each validation and test set. Furthermore, Table 3 shows the *Gini coefficient*  $C_G$  (Ceriani and Verme, 2011) of each fine-tuning test set, representing the level of class imbalance. The Gini coefficient provides a single bounded and interpretable scalar that quantifies the class imbalance, enabling a fair comparison across datasets with different numbers of classes.

<sup>1</sup> This is constrained by the class distribution and, consequently, on occasion, results in slightly lower or higher values. These values are generated to meet the criterion of maximizing the class overlap across all three subsets.

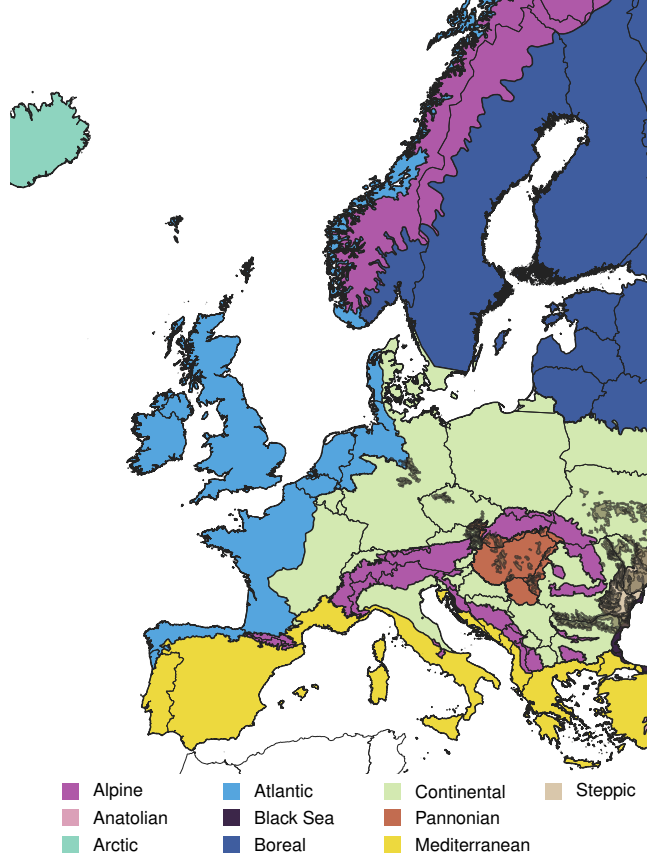


Figure 5. Biogeographical regions present in EUROCRoPSML 2.0, as defined by the (European Environment Agency (EEA), 2016).

We evaluate various few-shot settings with 1, 5, 10, 20, or 100 shots (*cf.* Reuss et al., 2025, 2026a) in order to determine the performance impact of the prior adjustment across different degrees of prior shifts. For each country, we compared the class distributions between the few-shot training set and the final test set to gauge the extent of the prior shift. In particular, we calculated the *Bhattacharyya distance*  $D_B$  (Bhattacharyya, 1946) to quantify the statistical overlap between crop classes, as shown in Table 4.

## 4. Methodology

We adopt the DirPA method (Reuss et al., 2026a), where class-prior uncertainty is modeled via a symmetric Dirichlet distribution and injected into the classifier logits during the training process.

### 4.1. DirPA: Dirichlet prior augmentation

Let  $f_\theta$  be a model parameterized by  $\theta$  and let  $z_i = f_\theta(x_i) \in \mathbb{R}^K$  denote logits for sample  $x_i$  over  $K$  classes. At each iteration  $s$ , a pseudo-prior

$$\tilde{\pi}^{(s)} \sim \text{Dir}(\alpha \cdot \mathbf{1}), \quad \tilde{\pi}^{(s)} \in \Delta^{K-1},$$

Table 2. Fine-tuning class distribution of EUROcropsML 2.0, showing the number of distinct crop classes. The total number of classes in the training set equals the number of available crop types and can be extracted from Table 1.

Country	# Crop classes			
	Train \ (validation $\cup$ test)	Validation	Test	Validation $\cap$ test
Belgium	2	133	133	132
Estonia	15	107	108	103
Latvia	2	106	105	105
Lithuania	0	22	22	22
Portugal	10	72	71	69
Slovakia	10	107	107	103
Slovenia	5	105	105	103
Spain	0	9	9	9

Table 3. Gini coefficient for the test sets of the EUROcropsML 2.0 fine-tuning countries, a measure of dataset skewness. A value of 0 indicates a perfectly balanced class distribution, while a value approaching 1 means almost all samples belong to a single majority class.

Country	Gini coefficient $C_G$
Belgium	0.939
Estonia	0.919
Latvia	0.910
Lithuania	0.761
Portugal	0.881
Slovakia	0.904
Slovenia	0.928
Spain	0.634

is sampled from the symmetric Dirichlet distribution defined over the  $(K - 1)$ -dimensional simplex  $\Delta^{K-1} = \{\boldsymbol{\pi} \in \mathbb{R}^K : \sum_{c=1}^K \pi_c = 1, \pi_c \geq 0\}$ . The parameter  $\alpha \in \mathbb{R}_+$  controls the degree of imbalance. A small value ( $\alpha < 1$ ) samples highly skewed (imbalanced) distributions, while  $\alpha \geq 1$  samples distributions closer to uniform, as visualized in Figure 6. The sampled prior is incorporated through a logit adjustment,

$$\mathbf{z}'_i \leftarrow \mathbf{z}_i + \tau \log(\tilde{\boldsymbol{\pi}}^{(s)}),$$

with  $\tau \in \mathbb{R}_+$  being a scaling factor. The modified logits  $\mathbf{z}'_i$  are subsequently passed through the *Softmax* function to obtain class probabilities

$$\hat{p}_{i,c} = \sigma(\mathbf{z}'_{i,c}) = \frac{\exp(\mathbf{z}'_{i,c})}{\sum_{k=1}^K \exp(\mathbf{z}'_{i,k})}, \quad c = 1, \dots, K.$$

Figure 7 illustrates the sampling process for  $K = 5$  classes and different values of  $\alpha$ .

#### 4.2. Transformer model

In alignment with Reuss et al. (2026a), all experiments from Section 5 are conducted using a state-of-the-art Transformer encoder architecture (Vaswani et al., 2017) stacked with a linear classification layer on top. To encode the temporal information, we apply sinusoidal positional encodings with a maximum sequence length of  $T_{\max} = 366$  days, representing a full leap year. While the encoder serves as the model’s feature extractor, the linear layer maps these features to the final class log-probabilities. We refer to the encoder

$$f_{\boldsymbol{\theta}_{\text{backbone}}}^{\text{backbone}} : \mathbb{R}^{T_{\max} \times d} \rightarrow \mathbb{R}^{n_e}$$

Table 4. Bhattacharyya distance for fine-tuning countries in EUROcropsML 2.0, calculated between the fixed test set and the few-shot training sets. The distance is 0 if the two distributions are identical and increases as they become more distinct.

Country	$k$ -shot training set				
	1	5	10	20	100
Belgium	0.880	0.850	0.827	0.786	0.637
Estonia	0.857	0.740	0.691	0.629	0.450
Latvia	0.736	0.716	0.688	0.655	0.539
Lithuania	0.365	0.365	0.365	0.365	0.365
Portugal	0.705	0.588	0.552	0.495	0.370
Slovakia	0.773	0.680	0.645	0.605	0.462
Slovenia	0.866	0.804	0.782	0.750	0.621
Spain	0.213	0.213	0.213	0.213	0.213

#### Algorithm 1 Dirichlet Prior Augmentation

**Require:**  $\alpha, \tau \in \mathbb{R}_+$

**Require:**  $\sigma(\cdot)$  (Softmax activation function)

**Require:**  $f_{\boldsymbol{\theta}}$  (model parameterized by  $\boldsymbol{\theta}$ )

```

1: for each training step  $s = 1$  to  $S$  do
2:   sample mini-batch of data points  $\mathcal{D}^{(s)} = \{(\mathbf{x}_i, y_i)\}_{i=1}^b$ 
3:   sample pseudo-prior  $\tilde{\boldsymbol{\pi}}^{(s)} \sim \text{Dir}(\alpha \cdot \mathbf{1})$ 
4:   for each data point  $(\mathbf{x}_i, y_i)$  in  $\mathcal{D}^{(s)}$  do
5:     compute base logits:  $\mathbf{z}_i \leftarrow f_{\boldsymbol{\theta}}(\mathbf{x}_i)$ 
6:     adjust logits:  $\mathbf{z}'_i \leftarrow \mathbf{z}_i + \tau \log(\tilde{\boldsymbol{\pi}}^{(s)})$ 
7:     compute predictive distribution:  $\hat{\mathbf{p}}_i \leftarrow \sigma(\mathbf{z}'_i)$ 
8:   end for
9:   compute mini-batch loss  $\mathcal{L}_{\text{batch}} \leftarrow \frac{1}{b} \sum_{i=1}^b \mathcal{L}(\hat{\mathbf{p}}_i, y_i)$ 
10:  update  $\boldsymbol{\theta}$  via backpropagation
11: end for

```

as the *backbone* and to the classification layer

$$f_{\boldsymbol{\theta}_{\text{head}}}^{\text{head}} : \mathbb{R}^{n_e} \rightarrow \mathbb{R}^K$$

as the *head*.  $d \in \{1, \dots, 13\}$  denotes the number of bands,  $n_e \in \mathbb{N}$  the Transformer’s embedding dimension, and  $\boldsymbol{\theta}_{\text{backbone}}$  the backbone’s and  $\boldsymbol{\theta}_{\text{head}}$  the head’s trainable parameter.

Subsequently, the full model is decomposed as

$$f_{\boldsymbol{\theta}} = f_{\boldsymbol{\theta}_{\text{head}}}^{\text{head}} \circ f_{\boldsymbol{\theta}_{\text{backbone}}}^{\text{backbone}},$$

where  $\boldsymbol{\theta} = [\boldsymbol{\theta}_{\text{backbone}}, \boldsymbol{\theta}_{\text{head}}]$  represents all trainable model parameters.

## 5. Experiments

Across all experiments, we employ a standard Transformer encoder consisting of four layers. Each layer features eight attention heads and a feed-forward network with a hidden layer of dimension 1024. Initially, input tokens are projected into a latent space of dimension 256 using internal embeddings. Regarding the spectral resolution, we retain 12 of the 13 Sentinel-2 bands, excluding B10 (cirrus), which is utilized solely for cloud detection during pre-processing, cf. Section 3. To obtain reflectance values, the raw data is normalized by a factor of  $10^4$ . The resulting values are clipped to the range  $[0.0, 1.2]$  and subsequently adjusted by an offset of  $10^{-4}$ . *No-data* values are either masked

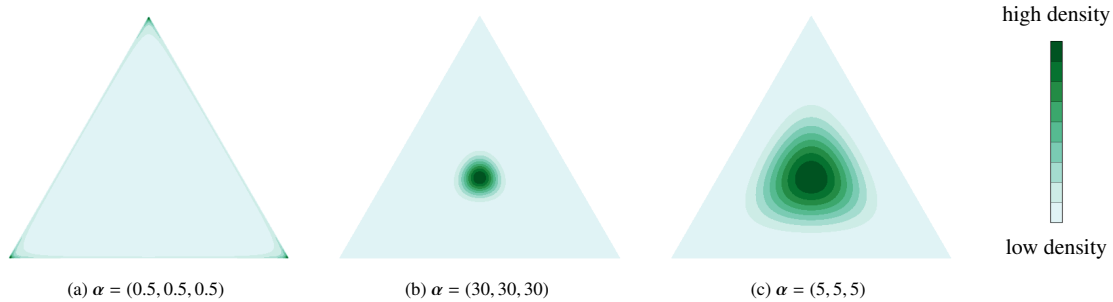


Figure 6. Dirichlet density for  $K = 3$  classes, defined over the  $(K - 1) = 2$ -simplex. The plots show different concentration parameters  $\alpha = \alpha \cdot \mathbf{1}$ , where  $\mathbf{1} = (1, 1, 1)^\top$  (Reuss et al., 2026a).

out or set to 0.0. For both pre-training and fine-tuning, all hyperparameters are optimized on the respective validation set. For the tuning trial runs, we employ a multi-variate *Bayesian tree-Parzen estimator (TPE)* with percentile pruning within the Optuna framework (Akiba et al., 2019).

All code used for training and evaluation will be made available upon publication.

### 5.1. Pre-training

First, we pre-train the model using downsampled parcel-level data from Austria and Germany. We downsample all 226 distinct crop classes to at most 10 000 samples per class. If fewer samples are available for a given class, all available samples are retained for that class. We use the standard *cross-entropy loss (CE)* with label smoothing and one cosine annealing cycle. We train the model for a total of 100 epochs and validate after each epoch on the full pre-training validation set. If the validation loss does not decrease for more than 15 epochs, we stop training. For details on hyperparameter tuning, please refer to Appendix B.1.

### 5.2. Fine-tuning

Pre-training is followed by fine-tuning on each of the remaining EURO-CROPSML 2.0 countries separately. For each fine-tuning case, we reinitialize the linear head  $f^{\text{head}}$  with the number of fine-tuning classes, cf. Table 1. For all experiments, we train for up to 200 epochs with a batch size of 16. Training is terminated if the validation loss fails to improve for 20 consecutive epochs. We use *Cohen’s kappa*  $\kappa$  evaluated on the validation set as the primary criterion for checkpoint selection, prioritizing models with robust inter-class reliability. This model state is then evaluated on the held-out test set. As a chance-corrected metric,  $\kappa$  ensures that the selected hyperparameters (cf. Appendix B.2) and checkpoints reflect genuine discriminative performance across all classes, particularly in the presence of significant class imbalance. This approach mitigates the accuracy paradox, in which high overall performance can be misleadingly achieved by frequent exploitation of the majority class. All fine-tuning experiments are conducted a total of five times with different random seeds  $r \in \{0, 1, 42, 123, 1234\}$ . The chosen random seed influences, for instance, the initialization of random parameters and mini-batch sampling. We conduct all fine-tuning experiments with both cross-entropy loss and focal loss (without a class-imbalance factor) in order to validate DirPA across varying

optimization landscapes. By utilizing FL, we can analyze the synergy between Dirichlet priors and difficulty-awareness. Both loss functions are trained with and without Dirichlet priors. We append the postfix ‘DirPA’ whenever the DirPA method is used.

## 6. Results

Cohen’s kappa serves as our main validation and evaluation metric. In addition, in order to analyze the trade-off between overall system robustness, overall performance, and class-specific performance, we also report *overall classification accuracy*  $a_{\text{OA}}$  (micro-averaged) and *F1-score* (macro-averaged). Tables 5 to 12 show the test metrics for each country and algorithm. The postfix DirPA is appended to the name of the loss function if the DirPA method has been utilized. All test metrics are reported using the best-performing model, measured by validation kappa. In addition to the most-granular classification results on HCAT level 6, we also report test accuracies and F1-scores on broader land cover classes (HCAT level 3). Predictions at level 3 are derived by mapping the predicted level 6 crop type to its corresponding parent category within the hierarchical structure. Furthermore, a visual representation of performance gains in relation to a country’s Gini coefficient (cf. Table 3) and the Bhattacharyya distance between the test set and each few-shot training set (cf. Table 4) is shown in Figures 8 and 9.

### Belgium Table 5a shows the classification results in Belgium.

Across all few-shot settings, the combination of CE DirPA consistently outperforms the baseline (and all other methods) in both Cohen’s kappa and overall accuracy. For kappa, DirPA achieves a relative performance gain of up to 33% (5-shot), maintaining a steady improvement of 9% even in the 100-shot. Furthermore, it also achieves the highest F1-scores for 1- and 5-shot. While FL with prior augmentation generally improves performance, it falls short of the baseline in the 5-shot benchmark, though it remains effective for F1-scores for 10- and 100-shot. Notably, while the FL baseline usually performs worse than the CE baseline, adding DirPA allows it to surpass the CE baseline in several scenarios. In terms of broader parent-level metrics, presented in Table 5b, DirPA again shows superior performance for accuracy and F1-score when paired with CE. When incorporated into FL, it, however, often falls short in terms of F1-scores, compared to its baseline.

Table 5. Few-shot classification results for **Belgium**. We show the results for the most-granular crop types, as presented in Table 2, as well as for the broader land cover classes (HCAT level 3). We report the metrics’ means  $\pm$  standard deviations on the test set for each variant and few-shot task, computed over five runs, cf. Section 5. The best result for each few-shot scenario is highlighted in **bold blue**. Depending on which loss function achieves the best result, the top result of the other loss function is shown in **bold black**.

(a) Fine-grained classification results on HCAT level 6.

Algorithm/Loss		Benchmark task ( $k$ -shot)				
		1	5	10	20	100
Kappa	CE	0.170 $\pm$ 0.011	0.278 $\pm$ 0.029	0.403 $\pm$ 0.040	0.462 $\pm$ 0.015	0.545 $\pm$ 0.012
	FL	0.156 $\pm$ 0.020	<b>0.268 <math>\pm</math> 0.020</b>	0.378 $\pm$ 0.030	0.435 $\pm$ 0.023	0.508 $\pm$ 0.025
	CE DirPA	<b>0.221 <math>\pm</math> 0.010</b>	<b>0.371 <math>\pm</math> 0.039</b>	<b>0.492 <math>\pm</math> 0.052</b>	<b>0.530 <math>\pm</math> 0.040</b>	<b>0.597 <math>\pm</math> 0.027</b>
	FL DirPA	<b>0.176 <math>\pm</math> 0.036</b>	0.248 $\pm$ 0.053	<b>0.405 <math>\pm</math> 0.028</b>	<b>0.439 <math>\pm</math> 0.063</b>	<b>0.536 <math>\pm</math> 0.022</b>
Accuracy	CE	0.185 $\pm$ 0.013	0.333 $\pm$ 0.053	0.480 $\pm$ 0.058	0.546 $\pm$ 0.019	0.627 $\pm$ 0.014
	FL	0.170 $\pm$ 0.022	<b>0.325 <math>\pm</math> 0.041</b>	0.462 $\pm$ 0.041	0.513 $\pm$ 0.027	0.594 $\pm$ 0.023
	CE DirPA	<b>0.254 <math>\pm</math> 0.040</b>	<b>0.469 <math>\pm</math> 0.044</b>	<b>0.589 <math>\pm</math> 0.061</b>	<b>0.625 <math>\pm</math> 0.049</b>	<b>0.687 <math>\pm</math> 0.025</b>
	FL DirPA	<b>0.194 <math>\pm</math> 0.039</b>	0.282 $\pm$ 0.075	<b>0.478 <math>\pm</math> 0.038</b>	<b>0.520 <math>\pm</math> 0.064</b>	<b>0.619 <math>\pm</math> 0.022</b>
F1-score	CE	0.084 $\pm$ 0.007	0.124 $\pm$ 0.018	<b>0.149 <math>\pm</math> 0.010</b>	<b>0.179 <math>\pm</math> 0.017</b>	<b>0.236 <math>\pm</math> 0.010</b>
	FL	<b>0.085 <math>\pm</math> 0.007</b>	<b>0.121 <math>\pm</math> 0.017</b>	0.140 $\pm$ 0.016	<b>0.182 <math>\pm</math> 0.010</b>	0.221 $\pm$ 0.024
	CE DirPA	<b>0.087 <math>\pm</math> 0.006</b>	<b>0.128 <math>\pm</math> 0.015</b>	0.144 $\pm$ 0.017	0.161 $\pm$ 0.025	0.215 $\pm$ 0.029
	FL DirPA	0.081 $\pm$ 0.007	0.121 $\pm$ 0.023	<b>0.146 <math>\pm</math> 0.012</b>	0.175 $\pm$ 0.018	<b>0.232 <math>\pm</math> 0.019</b>

(b) Classification results on HCAT level 3.

Algorithm/Loss		Benchmark task ( $k$ -shot)				
		1	5	10	20	100
Accuracy	CE	0.397 $\pm$ 0.015	0.488 $\pm$ 0.072	0.609 $\pm$ 0.058	0.664 $\pm$ 0.021	0.720 $\pm$ 0.015
	FL	0.390 $\pm$ 0.004	<b>0.492 <math>\pm</math> 0.060</b>	<b>0.613 <math>\pm</math> 0.041</b>	0.631 $\pm$ 0.024	0.700 $\pm$ 0.018
	CE DirPA	<b>0.422 <math>\pm</math> 0.074</b>	<b>0.618 <math>\pm</math> 0.047</b>	<b>0.710 <math>\pm</math> 0.052</b>	<b>0.738 <math>\pm</math> 0.050</b>	<b>0.785 <math>\pm</math> 0.023</b>
	FL DirPA	<b>0.392 <math>\pm</math> 0.007</b>	0.436 $\pm$ 0.074	0.592 $\pm$ 0.041	<b>0.648 <math>\pm</math> 0.041</b>	<b>0.720 <math>\pm</math> 0.020</b>
F1-score	CE	<b>0.167 <math>\pm</math> 0.018</b>	0.202 $\pm$ 0.034	0.280 $\pm$ 0.006	0.341 $\pm$ 0.025	<b>0.458 <math>\pm</math> 0.037</b>
	FL	<b>0.157 <math>\pm</math> 0.012</b>	<b>0.205 <math>\pm</math> 0.038</b>	<b>0.278 <math>\pm</math> 0.015</b>	<b>0.335 <math>\pm</math> 0.048</b>	0.403 $\pm$ 0.070
	CE DirPA	0.161 $\pm$ 0.038	<b>0.242 <math>\pm</math> 0.039</b>	<b>0.297 <math>\pm</math> 0.022</b>	<b>0.351 <math>\pm</math> 0.018</b>	0.422 $\pm$ 0.036
	FL DirPA	0.155 $\pm$ 0.015	0.173 $\pm$ 0.055	0.274 $\pm$ 0.014	0.327 $\pm$ 0.033	<b>0.435 <math>\pm</math> 0.049</b>

Table 6. Few-shot classification results for **Estonia**. We show the results for the most-granular crop types, as presented in Table 2, as well as for the broader land cover classes (HCAT level 3). We report the metrics’ means  $\pm$  standard deviations on the test set for each variant and few-shot task, computed over five runs, cf. Section 5. The best result for each few-shot scenario is highlighted in **bold blue**. Depending on which loss function achieves the best result, the top result of the other loss function is shown in **bold black**.

(a) Fine-grained classification results on HCAT level 6.

Algorithm/Loss		Benchmark task ( $k$ -shot)				
		1	5	10	20	100
Kappa	CE	0.200 $\pm$ 0.035	0.275 $\pm$ 0.013	0.334 $\pm$ 0.017	0.383 $\pm$ 0.016	0.487 $\pm$ 0.018
	FL	<b>0.198 <math>\pm</math> 0.029</b>	0.241 $\pm$ 0.021	0.308 $\pm$ 0.028	0.372 $\pm$ 0.035	0.473 $\pm$ 0.026
	CE DirPA	<b>0.306 <math>\pm</math> 0.060</b>	<b>0.401 <math>\pm</math> 0.037</b>	<b>0.448 <math>\pm</math> 0.032</b>	<b>0.479 <math>\pm</math> 0.025</b>	<b>0.532 <math>\pm</math> 0.008</b>
	FL DirPA	0.188 $\pm$ 0.059	<b>0.295 <math>\pm</math> 0.035</b>	<b>0.349 <math>\pm</math> 0.089</b>	<b>0.379 <math>\pm</math> 0.040</b>	<b>0.484 <math>\pm</math> 0.029</b>
Accuracy	CE	0.268 $\pm$ 0.061	0.350 $\pm$ 0.023	0.420 $\pm$ 0.030	0.479 $\pm$ 0.034	0.575 $\pm$ 0.020
	FL	<b>0.268 <math>\pm</math> 0.049</b>	0.311 $\pm$ 0.034	0.384 $\pm$ 0.040	0.465 $\pm$ 0.053	0.565 $\pm$ 0.029
	CE DirPA	<b>0.436 <math>\pm</math> 0.090</b>	<b>0.529 <math>\pm</math> 0.044</b>	<b>0.570 <math>\pm</math> 0.047</b>	<b>0.601 <math>\pm</math> 0.025</b>	<b>0.640 <math>\pm</math> 0.026</b>
	FL DirPA	0.252 $\pm$ 0.111	<b>0.380 <math>\pm</math> 0.060</b>	<b>0.441 <math>\pm</math> 0.137</b>	<b>0.483 <math>\pm</math> 0.071</b>	<b>0.580 <math>\pm</math> 0.035</b>
F1-score	CE	0.049 $\pm$ 0.005	<b>0.094 <math>\pm</math> 0.005</b>	<b>0.115 <math>\pm</math> 0.005</b>	<b>0.117 <math>\pm</math> 0.024</b>	<b>0.174 <math>\pm</math> 0.009</b>
	FL	0.048 $\pm$ 0.004	0.086 $\pm$ 0.009	<b>0.110 <math>\pm</math> 0.013</b>	<b>0.112 <math>\pm</math> 0.013</b>	<b>0.155 <math>\pm</math> 0.018</b>
	CE DirPA	<b>0.050 <math>\pm</math> 0.007</b>	0.078 $\pm$ 0.019	0.101 $\pm$ 0.016	0.095 $\pm$ 0.004	0.127 $\pm$ 0.029
	FL DirPA	<b>0.049 <math>\pm</math> 0.003</b>	<b>0.089 <math>\pm</math> 0.014</b>	0.094 $\pm$ 0.015	0.099 $\pm$ 0.027	0.140 $\pm$ 0.036

(b) Classification results on HCAT level 3.

Algorithm/Loss		Benchmark task ( $k$ -shot)				
		1	5	10	20	100
Accuracy	CE	0.577 $\pm$ 0.058	0.623 $\pm$ 0.029	0.669 $\pm$ 0.042	0.706 $\pm$ 0.039	0.760 $\pm$ 0.018
	FL	<b>0.579 <math>\pm</math> 0.054</b>	0.599 $\pm$ 0.045	0.637 $\pm$ 0.036	0.693 $\pm$ 0.049	0.757 $\pm$ 0.028
	CE DirPA	<b>0.730 <math>\pm</math> 0.066</b>	<b>0.757 <math>\pm</math> 0.041</b>	<b>0.785 <math>\pm</math> 0.034</b>	<b>0.812 <math>\pm</math> 0.032</b>	<b>0.816 <math>\pm</math> 0.021</b>
	FL DirPA	0.567 $\pm$ 0.115	<b>0.643 <math>\pm</math> 0.047</b>	<b>0.676 <math>\pm</math> 0.127</b>	<b>0.717 <math>\pm</math> 0.079</b>	<b>0.776 <math>\pm</math> 0.039</b>
F1-score	CE	0.209 $\pm$ 0.026	0.233 $\pm$ 0.014	0.261 $\pm$ 0.017	0.272 $\pm$ 0.014	0.307 $\pm$ 0.007
	FL	<b>0.213 <math>\pm</math> 0.027</b>	0.219 $\pm$ 0.022	0.243 $\pm$ 0.013	0.266 $\pm$ 0.021	0.303 $\pm$ 0.006
	CE DirPA	<b>0.273 <math>\pm</math> 0.022</b>	<b>0.287 <math>\pm</math> 0.012</b>	<b>0.299 <math>\pm</math> 0.014</b>	<b>0.311 <math>\pm</math> 0.011</b>	<b>0.313 <math>\pm</math> 0.016</b>
	FL DirPA	0.197 $\pm$ 0.061	<b>0.242 <math>\pm</math> 0.021</b>	<b>0.253 <math>\pm</math> 0.063</b>	<b>0.271 <math>\pm</math> 0.028</b>	<b>0.308 <math>\pm</math> 0.011</b>

Table 7. Few-shot classification results for **Latvia**. We show the results for the most-granular crop types, as presented in Table 2, as well as for the broader land cover classes (HCAT level 3). We report the metrics’ means  $\pm$  standard deviations on the test set for each variant and few-shot task, computed over five runs, cf. Section 5. The best result for each few-shot scenario is highlighted in **bold blue**. Depending on which loss function achieves the best result, the top result of the other loss function is shown in **bold black**.

(a) Fine-grained classification results on HCAT level 6.

Algorithm/Loss		Benchmark task ( $k$ -shot)				
		1	5	10	20	100
Kappa	CE	0.141 $\pm$ 0.012	<b>0.243 <math>\pm</math> 0.031</b>	0.251 $\pm$ 0.023	0.290 $\pm$ 0.024	<b>0.417 <math>\pm</math> 0.025</b>
	FL	0.155 $\pm$ 0.022	0.244 $\pm$ 0.059	0.243 $\pm$ 0.058	0.306 $\pm$ 0.023	0.397 $\pm$ 0.025
	CE DirPA	<b>0.143 <math>\pm</math> 0.025</b>	0.243 $\pm$ 0.017	<b>0.263 <math>\pm</math> 0.057</b>	<b>0.306 <math>\pm</math> 0.041</b>	0.411 $\pm$ 0.053
	FL DirPA	<b>0.204 <math>\pm</math> 0.055</b>	<b>0.345 <math>\pm</math> 0.077</b>	<b>0.339 <math>\pm</math> 0.057</b>	<b>0.384 <math>\pm</math> 0.061</b>	<b>0.424 <math>\pm</math> 0.029</b>
Accuracy	CE	0.187 $\pm$ 0.031	<b>0.305 <math>\pm</math> 0.052</b>	0.312 $\pm$ 0.035	0.337 $\pm$ 0.029	0.485 $\pm$ 0.028
	FL	0.214 $\pm$ 0.039	0.307 $\pm$ 0.090	0.304 $\pm$ 0.088	0.367 $\pm$ 0.034	0.464 $\pm$ 0.028
	CE DirPA	<b>0.197 <math>\pm</math> 0.043</b>	0.304 $\pm$ 0.027	<b>0.333 <math>\pm</math> 0.092</b>	<b>0.372 <math>\pm</math> 0.067</b>	<b>0.490 <math>\pm</math> 0.071</b>
	FL DirPA	<b>0.290 <math>\pm</math> 0.087</b>	<b>0.442 <math>\pm</math> 0.104</b>	<b>0.442 <math>\pm</math> 0.075</b>	<b>0.477 <math>\pm</math> 0.074</b>	<b>0.503 <math>\pm</math> 0.032</b>
F1-score	CE	<b>0.048 <math>\pm</math> 0.004</b>	0.089 $\pm$ 0.008	<b>0.100 <math>\pm</math> 0.007</b>	<b>0.130 <math>\pm</math> 0.004</b>	<b>0.168 <math>\pm</math> 0.005</b>
	FL	<b>0.047 <math>\pm</math> 0.006</b>	0.081 $\pm$ 0.004	<b>0.097 <math>\pm</math> 0.009</b>	<b>0.125 <math>\pm</math> 0.023</b>	<b>0.166 <math>\pm</math> 0.007</b>
	CE DirPA	0.047 $\pm$ 0.005	<b>0.092 <math>\pm</math> 0.011</b>	0.087 $\pm$ 0.014	0.116 $\pm$ 0.022	0.137 $\pm$ 0.031
	FL DirPA	0.042 $\pm$ 0.009	<b>0.088 <math>\pm</math> 0.009</b>	0.088 $\pm$ 0.015	0.107 $\pm$ 0.012	0.145 $\pm$ 0.015

(b) Classification results on HCAT level 3.

Algorithm/Loss		Benchmark task ( $k$ -shot)				
		1	5	10	20	100
Accuracy	CE	0.559 $\pm$ 0.037	<b>0.634 <math>\pm</math> 0.045</b>	0.637 $\pm$ 0.032	0.615 $\pm$ 0.028	<b>0.731 <math>\pm</math> 0.020</b>
	FL	0.579 $\pm$ 0.023	0.627 $\pm$ 0.090	0.613 $\pm$ 0.072	0.652 $\pm$ 0.037	0.715 $\pm$ 0.019
	CE DirPA	<b>0.568 <math>\pm</math> 0.053</b>	0.623 $\pm$ 0.033	<b>0.656 <math>\pm</math> 0.073</b>	<b>0.653 <math>\pm</math> 0.068</b>	0.731 $\pm$ 0.058
	FL DirPA	<b>0.626 <math>\pm</math> 0.065</b>	<b>0.719 <math>\pm</math> 0.082</b>	<b>0.726 <math>\pm</math> 0.053</b>	<b>0.751 <math>\pm</math> 0.047</b>	<b>0.751 <math>\pm</math> 0.025</b>
F1-score	CE	0.238 $\pm$ 0.040	<b>0.296 <math>\pm</math> 0.033</b>	0.301 $\pm$ 0.021	0.283 $\pm$ 0.019	<b>0.377 <math>\pm</math> 0.010</b>
	FL	0.256 $\pm$ 0.024	0.295 $\pm$ 0.067	0.276 $\pm$ 0.051	0.311 $\pm$ 0.020	0.366 $\pm$ 0.017
	CE DirPA	<b>0.258 <math>\pm</math> 0.031</b>	0.293 $\pm$ 0.012	<b>0.302 <math>\pm</math> 0.050</b>	<b>0.306 <math>\pm</math> 0.038</b>	0.369 $\pm$ 0.021
	FL DirPA	<b>0.277 <math>\pm</math> 0.044</b>	<b>0.352 <math>\pm</math> 0.056</b>	<b>0.351 <math>\pm</math> 0.037</b>	<b>0.367 <math>\pm</math> 0.032</b>	<b>0.377 <math>\pm</math> 0.020</b>

Table 8. Few-shot classification results for **Lithuania**. We show the results for the most-granular crop types, as presented in Table 2, as well as for the broader land cover classes (HCAT level 3). We report the metrics’ means  $\pm$  standard deviations on the test set for each variant and few-shot task, computed over five runs, cf. Section 5. The best result for each few-shot scenario is highlighted in **bold blue**. Depending on which loss function achieves the best result, the top result of the other loss function is shown in **bold black**.

(a) Fine-grained classification results on HCAT level 6.

Algorithm/Loss		Benchmark task ( $k$ -shot)				
		1	5	10	20	100
Kappa	CE	0.337 $\pm$ 0.042	0.441 $\pm$ 0.021	0.470 $\pm$ 0.019	0.538 $\pm$ 0.022	0.606 $\pm$ 0.007
	FL	0.375 $\pm$ 0.042	0.456 $\pm$ 0.032	0.546 $\pm$ 0.046	0.577 $\pm$ 0.018	0.641 $\pm$ 0.019
	CE DirPA	<b>0.347 <math>\pm</math> 0.036</b>	<b>0.510 <math>\pm</math> 0.044</b>	<b>0.495 <math>\pm</math> 0.041</b>	<b>0.576 <math>\pm</math> 0.073</b>	<b>0.637 <math>\pm</math> 0.034</b>
	FL DirPA	<b>0.445 <math>\pm</math> 0.018</b>	<b>0.575 <math>\pm</math> 0.020</b>	<b>0.637 <math>\pm</math> 0.018</b>	<b>0.640 <math>\pm</math> 0.032</b>	<b>0.675 <math>\pm</math> 0.018</b>
Accuracy	CE	0.431 $\pm$ 0.061	0.525 $\pm$ 0.020	0.552 $\pm$ 0.029	0.614 $\pm$ 0.026	0.682 $\pm$ 0.005
	FL	0.479 $\pm$ 0.048	0.548 $\pm$ 0.043	0.632 $\pm$ 0.054	0.662 $\pm$ 0.026	0.719 $\pm$ 0.020
	CE DirPA	<b>0.436 <math>\pm</math> 0.040</b>	<b>0.606 <math>\pm</math> 0.042</b>	<b>0.579 <math>\pm</math> 0.041</b>	<b>0.653 <math>\pm</math> 0.074</b>	<b>0.710 <math>\pm</math> 0.033</b>
	FL DirPA	<b>0.565 <math>\pm</math> 0.028</b>	<b>0.668 <math>\pm</math> 0.020</b>	<b>0.730 <math>\pm</math> 0.009</b>	<b>0.724 <math>\pm</math> 0.030</b>	<b>0.747 <math>\pm</math> 0.018</b>
F1-score	CE	0.233 $\pm$ 0.036	<b>0.331 <math>\pm</math> 0.019</b>	<b>0.351 <math>\pm</math> 0.012</b>	0.398 $\pm$ 0.014	<b>0.432 <math>\pm</math> 0.011</b>
	FL	0.246 $\pm$ 0.041	0.329 $\pm$ 0.022	<b>0.360 <math>\pm</math> 0.015</b>	0.375 $\pm$ 0.039	0.431 $\pm$ 0.021
	CE DirPA	<b>0.248 <math>\pm</math> 0.028</b>	0.328 $\pm$ 0.025	0.345 $\pm$ 0.024	<b>0.401 <math>\pm</math> 0.023</b>	0.427 $\pm$ 0.025
	FL DirPA	<b>0.251 <math>\pm</math> 0.031</b>	<b>0.337 <math>\pm</math> 0.020</b>	0.335 $\pm$ 0.023	<b>0.384 <math>\pm</math> 0.015</b>	<b>0.437 <math>\pm</math> 0.021</b>

(b) Classification results on HCAT level 3.

Algorithm/Loss		Benchmark task ( $k$ -shot)				
		1	5	10	20	100
Accuracy	CE	0.685 $\pm$ 0.067	0.720 $\pm$ 0.021	0.719 $\pm$ 0.032	0.748 $\pm$ 0.035	0.809 $\pm$ 0.007
	FL	0.736 $\pm$ 0.039	0.757 $\pm$ 0.046	0.794 $\pm$ 0.065	0.808 $\pm$ 0.045	0.847 $\pm$ 0.028
	CE DirPA	<b>0.687 <math>\pm</math> 0.030</b>	<b>0.810 <math>\pm</math> 0.025</b>	<b>0.743 <math>\pm</math> 0.041</b>	<b>0.783 <math>\pm</math> 0.072</b>	<b>0.831 <math>\pm</math> 0.032</b>
	FL DirPA	<b>0.798 <math>\pm</math> 0.031</b>	<b>0.837 <math>\pm</math> 0.018</b>	<b>0.873 <math>\pm</math> 0.013</b>	<b>0.858 <math>\pm</math> 0.025</b>	<b>0.860 <math>\pm</math> 0.019</b>
F1-score	CE	0.264 $\pm$ 0.034	0.330 $\pm$ 0.009	0.324 $\pm$ 0.018	0.372 $\pm$ 0.029	0.431 $\pm$ 0.010
	FL	0.295 $\pm$ 0.019	0.345 $\pm$ 0.026	0.367 $\pm$ 0.038	0.393 $\pm$ 0.015	0.453 $\pm$ 0.014
	CE DirPA	<b>0.274 <math>\pm</math> 0.014</b>	<b>0.364 <math>\pm</math> 0.012</b>	<b>0.331 <math>\pm</math> 0.029</b>	<b>0.396 <math>\pm</math> 0.040</b>	<b>0.434 <math>\pm</math> 0.010</b>
	FL DirPA	<b>0.313 <math>\pm</math> 0.010</b>	<b>0.377 <math>\pm</math> 0.018</b>	<b>0.368 <math>\pm</math> 0.039</b>	<b>0.421 <math>\pm</math> 0.028</b>	<b>0.454 <math>\pm</math> 0.012</b>

Table 9. Few-shot classification results for **Portugal**. We show the results for the most-granular crop types, as presented in Table 2, as well as for the broader land cover classes (HCAT level 3). We report the metrics’ means  $\pm$  standard deviations on the test set for each variant and few-shot task, computed over five runs, cf. Section 5. The best result for each few-shot scenario is highlighted in **bold blue**. Depending on which loss function achieves the best result, the top result of the other loss function is shown in **bold black**.

(a) Fine-grained classification results on HCAT level 6.

Algorithm/Loss		Benchmark task ( $k$ -shot)				
		1	5	10	20	100
Kappa	CE	<b>0.049 <math>\pm</math> 0.003</b>	0.092 $\pm$ 0.008	0.126 $\pm$ 0.006	0.165 $\pm$ 0.011	<b>0.286 <math>\pm</math> 0.017</b>
	FL	0.043 $\pm$ 0.008	<b>0.083 <math>\pm</math> 0.005</b>	0.130 $\pm$ 0.009	0.168 $\pm$ 0.018	0.262 $\pm$ 0.018
	CE DirPA	0.049 $\pm$ 0.006	<b>0.097 <math>\pm</math> 0.007</b>	<b>0.130 <math>\pm</math> 0.010</b>	<b>0.176 <math>\pm</math> 0.011</b>	0.282 $\pm$ 0.012
	FL DirPA	<b>0.055 <math>\pm</math> 0.012</b>	0.082 $\pm$ 0.002	<b>0.137 <math>\pm</math> 0.010</b>	<b>0.181 <math>\pm</math> 0.004</b>	<b>0.280 <math>\pm</math> 0.017</b>
Accuracy	CE	0.070 $\pm$ 0.009	0.125 $\pm$ 0.015	0.162 $\pm$ 0.010	0.206 $\pm$ 0.009	<b>0.343 <math>\pm</math> 0.021</b>
	FL	0.063 $\pm$ 0.013	<b>0.114 <math>\pm</math> 0.008</b>	0.168 $\pm$ 0.011	0.217 $\pm$ 0.033	0.322 $\pm$ 0.017
	CE DirPA	<b>0.074 <math>\pm</math> 0.011</b>	<b>0.137 <math>\pm</math> 0.019</b>	<b>0.170 <math>\pm</math> 0.014</b>	<b>0.223 <math>\pm</math> 0.015</b>	0.342 $\pm$ 0.017
	FL DirPA	<b>0.085 <math>\pm</math> 0.024</b>	0.112 $\pm$ 0.007	<b>0.182 <math>\pm</math> 0.019</b>	<b>0.233 <math>\pm</math> 0.020</b>	<b>0.339 <math>\pm</math> 0.024</b>
F1-score	CE	<b>0.032 <math>\pm</math> 0.006</b>	<b>0.056 <math>\pm</math> 0.005</b>	0.070 $\pm$ 0.003	0.089 $\pm$ 0.008	<b>0.132 <math>\pm</math> 0.009</b>
	FL	<b>0.032 <math>\pm</math> 0.005</b>	<b>0.052 <math>\pm</math> 0.008</b>	0.071 $\pm$ 0.004	0.083 $\pm$ 0.010	0.130 $\pm$ 0.015
	CE DirPA	0.029 $\pm$ 0.009	0.052 $\pm$ 0.003	<b>0.073 <math>\pm</math> 0.004</b>	<b>0.093 <math>\pm</math> 0.004</b>	0.131 $\pm$ 0.011
	FL DirPA	0.028 $\pm$ 0.007	0.052 $\pm$ 0.008	<b>0.072 <math>\pm</math> 0.011</b>	<b>0.093 <math>\pm</math> 0.008</b>	<b>0.139 <math>\pm</math> 0.009</b>

(b) Classification results on HCAT level 3.

Algorithm/Loss		Benchmark task ( $k$ -shot)				
		1	5	10	20	100
Accuracy	CE	<b>0.313 <math>\pm</math> 0.005</b>	0.343 $\pm$ 0.012	0.375 $\pm$ 0.012	0.420 $\pm$ 0.026	0.520 $\pm$ 0.015
	FL	0.307 $\pm$ 0.017	<b>0.333 <math>\pm</math> 0.012</b>	0.387 $\pm$ 0.013	<b>0.432 <math>\pm</math> 0.045</b>	0.502 $\pm$ 0.022
	CE DirPA	0.308 $\pm$ 0.020	<b>0.361 <math>\pm</math> 0.011</b>	<b>0.394 <math>\pm</math> 0.011</b>	<b>0.436 <math>\pm</math> 0.019</b>	<b>0.522 <math>\pm</math> 0.016</b>
	FL DirPA	<b>0.312 <math>\pm</math> 0.033</b>	0.328 $\pm$ 0.021	<b>0.390 <math>\pm</math> 0.021</b>	0.429 $\pm$ 0.025	<b>0.511 <math>\pm</math> 0.020</b>
F1-score	CE	<b>0.245 <math>\pm</math> 0.010</b>	0.265 $\pm$ 0.008	0.297 $\pm$ 0.013	0.327 $\pm$ 0.025	<b>0.440 <math>\pm</math> 0.021</b>
	FL	0.234 $\pm$ 0.014	0.253 $\pm$ 0.012	0.310 $\pm$ 0.005	<b>0.348 <math>\pm</math> 0.049</b>	0.418 $\pm$ 0.023
	CE DirPA	0.229 $\pm$ 0.024	<b>0.279 <math>\pm</math> 0.013</b>	<b>0.314 <math>\pm</math> 0.015</b>	<b>0.359 <math>\pm</math> 0.012</b>	0.432 $\pm$ 0.013
	FL DirPA	<b>0.238 <math>\pm</math> 0.034</b>	<b>0.254 <math>\pm</math> 0.007</b>	<b>0.319 <math>\pm</math> 0.015</b>	0.347 $\pm$ 0.023	<b>0.419 <math>\pm</math> 0.018</b>

Table 10. Few-shot classification results for **Slovakia**. We show the results for the most-granular crop types, as presented in Table 2, as well as for the broader land cover classes (HCAT level 3). We report the metrics’ means  $\pm$  standard deviations on the test set for each variant and few-shot task, computed over five runs, cf. Section 5. The best result for each few-shot scenario is highlighted in **bold blue**. Depending on which loss function achieves the best result, the top result of the other loss function is shown in **bold black**.

(a) Fine-grained classification results on HCAT level 6.

Algorithm/Loss		Benchmark task ( $k$ -shot)				
		1	5	10	20	100
Kappa	CE	<b>0.185 <math>\pm</math> 0.009</b>	0.443 $\pm$ 0.021	0.455 $\pm$ 0.034	0.477 $\pm$ 0.027	0.565 $\pm$ 0.021
	FL	0.175 $\pm$ 0.008	0.418 $\pm$ 0.036	0.456 $\pm$ 0.021	0.458 $\pm$ 0.036	0.556 $\pm$ 0.015
	CE DirPA	0.182 $\pm$ 0.009	<b>0.465 <math>\pm</math> 0.031</b>	<b>0.462 <math>\pm</math> 0.038</b>	<b>0.527 <math>\pm</math> 0.034</b>	<b>0.579 <math>\pm</math> 0.010</b>
	FL DirPA	<b>0.177 <math>\pm</math> 0.019</b>	<b>0.449 <math>\pm</math> 0.046</b>	<b>0.464 <math>\pm</math> 0.036</b>	<b>0.510 <math>\pm</math> 0.024</b>	<b>0.578 <math>\pm</math> 0.025</b>
Accuracy	CE	<b>0.209 <math>\pm</math> 0.012</b>	0.520 $\pm$ 0.025	0.526 $\pm$ 0.038	0.558 $\pm$ 0.037	0.641 $\pm$ 0.025
	FL	0.197 $\pm$ 0.009	0.492 $\pm$ 0.045	0.535 $\pm$ 0.031	0.533 $\pm$ 0.041	0.632 $\pm$ 0.016
	CE DirPA	0.209 $\pm$ 0.013	<b>0.550 <math>\pm</math> 0.044</b>	<b>0.533 <math>\pm</math> 0.044</b>	<b>0.611 <math>\pm</math> 0.036</b>	<b>0.657 <math>\pm</math> 0.011</b>
	FL DirPA	<b>0.201 <math>\pm</math> 0.024</b>	<b>0.525 <math>\pm</math> 0.062</b>	<b>0.538 <math>\pm</math> 0.040</b>	<b>0.591 <math>\pm</math> 0.027</b>	<b>0.654 <math>\pm</math> 0.029</b>
F1-score	CE	<b>0.105 <math>\pm</math> 0.003</b>	0.159 $\pm$ 0.015	0.182 $\pm$ 0.009	<b>0.188 <math>\pm</math> 0.020</b>	<b>0.233 <math>\pm</math> 0.021</b>
	FL	<b>0.102 <math>\pm</math> 0.004</b>	0.154 $\pm$ 0.015	0.171 $\pm$ 0.014	0.188 $\pm$ 0.005	<b>0.221 <math>\pm</math> 0.019</b>
	CE DirPA	0.090 $\pm$ 0.023	<b>0.160 <math>\pm</math> 0.014</b>	<b>0.191 <math>\pm</math> 0.008</b>	0.188 $\pm$ 0.016	0.181 $\pm$ 0.021
	FL DirPA	0.087 $\pm$ 0.024	<b>0.163 <math>\pm</math> 0.012</b>	<b>0.184 <math>\pm</math> 0.016</b>	<b>0.195 <math>\pm</math> 0.011</b>	0.200 $\pm$ 0.035

(b) Classification results on HCAT level 3.

Algorithm/Loss		Benchmark task ( $k$ -shot)				
		1	5	10	20	100
Accuracy	CE	0.500 $\pm$ 0.030	0.754 $\pm$ 0.029	0.746 $\pm$ 0.028	0.783 $\pm$ 0.050	0.833 $\pm$ 0.032
	FL	0.496 $\pm$ 0.023	0.734 $\pm$ 0.041	<b>0.773 <math>\pm</math> 0.055</b>	0.755 $\pm$ 0.038	0.826 $\pm$ 0.016
	CE DirPA	<b>0.519 <math>\pm</math> 0.021</b>	<b>0.785 <math>\pm</math> 0.046</b>	<b>0.752 <math>\pm</math> 0.032</b>	<b>0.820 <math>\pm</math> 0.025</b>	<b>0.847 <math>\pm</math> 0.012</b>
	FL DirPA	<b>0.510 <math>\pm</math> 0.029</b>	<b>0.759 <math>\pm</math> 0.066</b>	0.768 $\pm$ 0.035	<b>0.806 <math>\pm</math> 0.028</b>	<b>0.839 <math>\pm</math> 0.030</b>
F1-score	CE	0.215 $\pm$ 0.007	0.358 $\pm$ 0.015	<b>0.340 <math>\pm</math> 0.021</b>	0.361 $\pm$ 0.037	0.423 $\pm$ 0.005
	FL	0.220 $\pm$ 0.002	0.335 $\pm$ 0.027	0.352 $\pm$ 0.039	0.346 $\pm$ 0.018	0.411 $\pm$ 0.014
	CE DirPA	<b>0.233 <math>\pm</math> 0.014</b>	<b>0.372 <math>\pm</math> 0.041</b>	0.340 $\pm$ 0.022	<b>0.389 <math>\pm</math> 0.035</b>	<b>0.428 <math>\pm</math> 0.031</b>
	FL DirPA	<b>0.221 <math>\pm</math> 0.013</b>	<b>0.367 <math>\pm</math> 0.053</b>	<b>0.361 <math>\pm</math> 0.015</b>	<b>0.385 <math>\pm</math> 0.027</b>	<b>0.422 <math>\pm</math> 0.035</b>

Table 11. Few-shot classification results for **Slovenia**. We show the results for the most-granular crop types, as presented in Table 2, as well as for the broader land cover classes (HCAT level 3). We report the metrics’ means  $\pm$  standard deviations on the test set for each variant and few-shot task, computed over five runs, cf. Section 5. The best result for each few-shot scenario is highlighted in **bold blue**. Depending on which loss function achieves the best result, the top result of the other loss function is shown in **bold black**.

(a) Fine-grained classification results on HCAT level 6.

Algorithm/Loss		Benchmark task ( $k$ -shot)				
		1	5	10	20	100
Kappa	CE	0.216 $\pm$ 0.032	0.198 $\pm$ 0.025	0.253 $\pm$ 0.012	0.288 $\pm$ 0.020	0.354 $\pm$ 0.018
	FL	0.218 $\pm$ 0.032	0.211 $\pm$ 0.014	0.262 $\pm$ 0.029	0.295 $\pm$ 0.011	0.347 $\pm$ 0.014
	CE DirPA	<b>0.287 <math>\pm</math> 0.032</b>	<b>0.314 <math>\pm</math> 0.050</b>	<b>0.345 <math>\pm</math> 0.025</b>	<b>0.388 <math>\pm</math> 0.038</b>	<b>0.412 <math>\pm</math> 0.014</b>
	FL DirPA	<b>0.300 <math>\pm</math> 0.030</b>	<b>0.318 <math>\pm</math> 0.037</b>	<b>0.327 <math>\pm</math> 0.037</b>	<b>0.381 <math>\pm</math> 0.044</b>	<b>0.405 <math>\pm</math> 0.022</b>
Accuracy	CE	0.305 $\pm$ 0.061	0.270 $\pm$ 0.041	0.338 $\pm$ 0.019	0.382 $\pm$ 0.028	0.456 $\pm$ 0.024
	FL	0.321 $\pm$ 0.060	0.294 $\pm$ 0.028	0.356 $\pm$ 0.046	0.401 $\pm$ 0.020	0.444 $\pm$ 0.019
	CE DirPA	<b>0.418 <math>\pm</math> 0.051</b>	<b>0.449 <math>\pm</math> 0.072</b>	<b>0.491 <math>\pm</math> 0.033</b>	<b>0.538 <math>\pm</math> 0.057</b>	<b>0.549 <math>\pm</math> 0.031</b>
	FL DirPA	<b>0.438 <math>\pm</math> 0.048</b>	<b>0.454 <math>\pm</math> 0.051</b>	<b>0.450 <math>\pm</math> 0.053</b>	<b>0.522 <math>\pm</math> 0.066</b>	<b>0.523 <math>\pm</math> 0.031</b>
F1-score	CE	0.071 $\pm$ 0.015	0.083 $\pm$ 0.006	<b>0.100 <math>\pm</math> 0.005</b>	<b>0.106 <math>\pm</math> 0.004</b>	<b>0.129 <math>\pm</math> 0.004</b>
	FL	0.068 $\pm$ 0.013	0.087 $\pm$ 0.004	<b>0.104 <math>\pm</math> 0.002</b>	0.099 $\pm$ 0.008	<b>0.136 <math>\pm</math> 0.010</b>
	CE DirPA	<b>0.074 <math>\pm</math> 0.014</b>	<b>0.087 <math>\pm</math> 0.008</b>	0.092 $\pm$ 0.005	0.106 $\pm$ 0.006	0.114 $\pm$ 0.020
	FL DirPA	<b>0.076 <math>\pm</math> 0.004</b>	<b>0.089 <math>\pm</math> 0.007</b>	0.099 $\pm$ 0.003	<b>0.101 <math>\pm</math> 0.006</b>	0.122 $\pm$ 0.010

(b) Classification results on HCAT level 3.

Algorithm/Loss		Benchmark task ( $k$ -shot)				
		1	5	10	20	100
Accuracy	CE	0.540 $\pm$ 0.053	0.511 $\pm$ 0.041	0.564 $\pm$ 0.018	0.596 $\pm$ 0.022	0.656 $\pm$ 0.022
	FL	0.558 $\pm$ 0.058	0.531 $\pm$ 0.038	0.588 $\pm$ 0.045	0.616 $\pm$ 0.023	0.642 $\pm$ 0.014
	CE DirPA	<b>0.633 <math>\pm</math> 0.036</b>	<b>0.674 <math>\pm</math> 0.070</b>	<b>0.711 <math>\pm</math> 0.030</b>	<b>0.727 <math>\pm</math> 0.053</b>	<b>0.728 <math>\pm</math> 0.034</b>
	FL DirPA	<b>0.640 <math>\pm</math> 0.043</b>	<b>0.669 <math>\pm</math> 0.061</b>	<b>0.662 <math>\pm</math> 0.050</b>	<b>0.716 <math>\pm</math> 0.056</b>	<b>0.697 <math>\pm</math> 0.028</b>
F1-score	CE	0.257 $\pm$ 0.030	0.245 $\pm$ 0.023	0.279 $\pm$ 0.006	0.287 $\pm$ 0.011	0.317 $\pm$ 0.009
	FL	0.267 $\pm$ 0.028	0.255 $\pm$ 0.019	0.289 $\pm$ 0.017	0.295 $\pm$ 0.013	0.311 $\pm$ 0.008
	CE DirPA	<b>0.295 <math>\pm</math> 0.016</b>	<b>0.315 <math>\pm</math> 0.027</b>	<b>0.336 <math>\pm</math> 0.007</b>	<b>0.340 <math>\pm</math> 0.019</b>	<b>0.343 <math>\pm</math> 0.013</b>
	FL DirPA	<b>0.295 <math>\pm</math> 0.014</b>	<b>0.314 <math>\pm</math> 0.023</b>	<b>0.316 <math>\pm</math> 0.018</b>	<b>0.333 <math>\pm</math> 0.021</b>	<b>0.334 <math>\pm</math> 0.012</b>

Table 12. Few-shot classification results for **Spain**. We show the results for the most-granular crop types, as presented in Table 2, as well as for the broader land cover classes (HCAT level 3). We report the metrics’ means  $\pm$  standard deviations on the test set for each variant and few-shot task, computed over five runs, cf. Section 5. The best result for each few-shot scenario is highlighted in **bold blue**. Depending on which loss function achieves the best result, the top result of the other loss function is shown in **bold black**.

(a) Fine-grained classification results on HCAT level 6.

Algorithm/Loss		Benchmark task ( $k$ -shot)				
		1	5	10	20	100
Kappa	CE	0.271 $\pm$ 0.011	0.325 $\pm$ 0.017	0.341 $\pm$ 0.020	0.400 $\pm$ 0.023	0.460 $\pm$ 0.013
	FL	0.284 $\pm$ 0.035	0.344 $\pm$ 0.026	<b>0.348 <math>\pm</math> 0.029</b>	0.405 $\pm$ 0.007	<b>0.466 <math>\pm</math> 0.026</b>
	CE DirPA	<b>0.341 <math>\pm</math> 0.014</b>	<b>0.356 <math>\pm</math> 0.020</b>	<b>0.354 <math>\pm</math> 0.012</b>	<b>0.422 <math>\pm</math> 0.009</b>	<b>0.462 <math>\pm</math> 0.004</b>
	FL DirPA	<b>0.331 <math>\pm</math> 0.030</b>	<b>0.349 <math>\pm</math> 0.027</b>	0.333 $\pm$ 0.030	<b>0.410 <math>\pm</math> 0.018</b>	0.453 $\pm$ 0.030
Accuracy	CE	0.403 $\pm$ 0.013	0.472 $\pm$ 0.023	0.493 $\pm$ 0.028	0.522 $\pm$ 0.026	0.583 $\pm$ 0.016
	FL	0.424 $\pm$ 0.047	0.490 $\pm$ 0.033	<b>0.498 <math>\pm</math> 0.049</b>	0.532 $\pm$ 0.011	<b>0.592 <math>\pm</math> 0.035</b>
	CE DirPA	<b>0.525 <math>\pm</math> 0.021</b>	<b>0.507 <math>\pm</math> 0.029</b>	<b>0.499 <math>\pm</math> 0.020</b>	<b>0.551 <math>\pm</math> 0.014</b>	<b>0.584 <math>\pm</math> 0.005</b>
	FL DirPA	<b>0.516 <math>\pm</math> 0.036</b>	<b>0.510 <math>\pm</math> 0.023</b>	0.469 $\pm$ 0.034	<b>0.542 <math>\pm</math> 0.017</b>	0.578 $\pm$ 0.033
F1-score	CE	0.247 $\pm$ 0.008	<b>0.292 <math>\pm</math> 0.014</b>	0.301 $\pm$ 0.014	0.340 $\pm$ 0.016	0.398 $\pm$ 0.007
	FL	<b>0.254 <math>\pm</math> 0.012</b>	<b>0.294 <math>\pm</math> 0.021</b>	0.299 $\pm$ 0.015	0.337 $\pm$ 0.009	<b>0.395 <math>\pm</math> 0.018</b>
	CE DirPA	<b>0.271 <math>\pm</math> 0.012</b>	0.289 $\pm$ 0.008	<b>0.305 <math>\pm</math> 0.013</b>	<b>0.353 <math>\pm</math> 0.004</b>	<b>0.399 <math>\pm</math> 0.007</b>
	FL DirPA	0.252 $\pm$ 0.027	0.277 $\pm$ 0.041	<b>0.310 <math>\pm</math> 0.020</b>	<b>0.340 <math>\pm</math> 0.014</b>	0.392 $\pm$ 0.019

(b) Classification results on HCAT level 3.

Algorithm/Loss		Benchmark task ( $k$ -shot)				
		1	5	10	20	100
Accuracy	CE	0.456 $\pm$ 0.014	0.518 $\pm$ 0.012	0.528 $\pm$ 0.014	0.566 $\pm$ 0.021	0.618 $\pm$ 0.013
	FL	0.476 $\pm$ 0.036	0.530 $\pm$ 0.032	<b>0.532 <math>\pm</math> 0.031</b>	0.577 $\pm$ 0.005	<b>0.627 <math>\pm</math> 0.025</b>
	CE DirPA	<b>0.555 <math>\pm</math> 0.020</b>	<b>0.539 <math>\pm</math> 0.019</b>	<b>0.541 <math>\pm</math> 0.015</b>	<b>0.596 <math>\pm</math> 0.007</b>	<b>0.626 <math>\pm</math> 0.007</b>
	FL DirPA	<b>0.537 <math>\pm</math> 0.028</b>	<b>0.538 <math>\pm</math> 0.030</b>	0.515 $\pm$ 0.018	<b>0.589 <math>\pm</math> 0.018</b>	0.612 $\pm$ 0.028
F1-score	CE	0.375 $\pm$ 0.009	0.417 $\pm$ 0.012	0.422 $\pm$ 0.012	0.462 $\pm$ 0.016	0.504 $\pm$ 0.007
	FL	0.389 $\pm$ 0.026	<b>0.419 <math>\pm</math> 0.021</b>	<b>0.427 <math>\pm</math> 0.017</b>	0.471 $\pm$ 0.003	<b>0.510 <math>\pm</math> 0.016</b>
	CE DirPA	<b>0.423 <math>\pm</math> 0.010</b>	<b>0.427 <math>\pm</math> 0.011</b>	<b>0.434 <math>\pm</math> 0.010</b>	<b>0.478 <math>\pm</math> 0.002</b>	<b>0.513 <math>\pm</math> 0.007</b>
	FL DirPA	<b>0.404 <math>\pm</math> 0.019</b>	0.416 $\pm$ 0.026	0.414 $\pm$ 0.013	<b>0.474 <math>\pm</math> 0.012</b>	0.500 $\pm$ 0.020

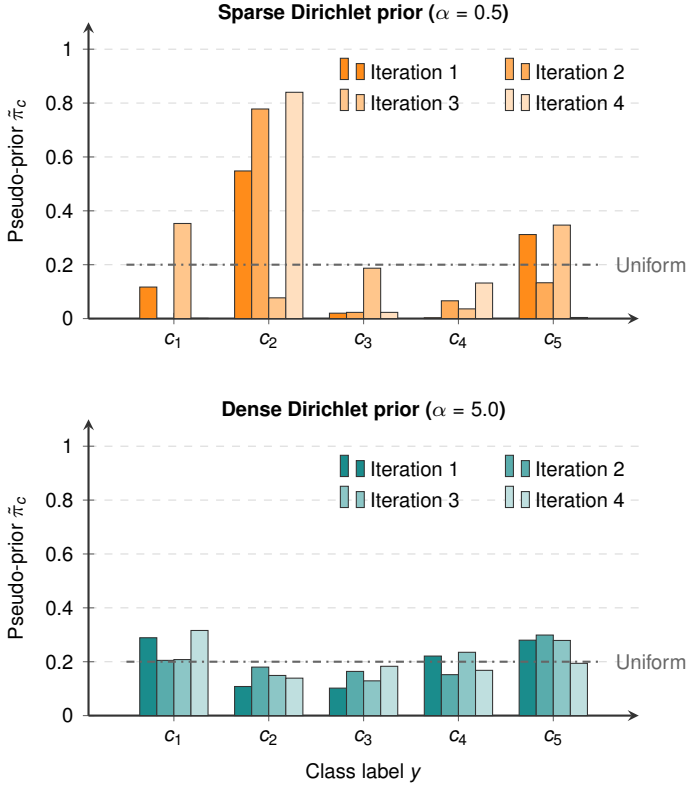


Figure 7. Visualization of four possible draws of the pseudo-prior  $\bar{\pi}^{(s)} \sim \text{Dir}(\alpha \cdot \mathbf{1})$  for  $K = 5$  classes at consecutive training iterations  $s$ . The orange sampling ( $\alpha = 0.5$ ) produces sparse draws, with a different class dominating at each iteration. With  $\alpha = 5$  (teal), the draws remain closer to the uniform distribution, indicated by the dashed line. Resampling the pseudo-prior at each iteration exposes the model to a diverse set of imbalance patterns without assuming any fixed test distribution.

**Estonia** Again, when combined with CE, DirPA shows consistent superior performance compared to the CE baseline (and all other options) in terms of kappa and accuracy (Table 6a). The highest relative performance gain in kappa even reaches 45% (1-shot), with gains again persisting at 9% even in the 100-shot case. For 1-shot, it surpasses the remaining methods in terms of F1-score. For the combination of FL and prior augmentation, we can observe a similar pattern to the one in Belgium, where DirPA enables FL to often surpass the CE baseline in terms of kappa and accuracy. Furthermore, for 5-shot, it improves all three metrics compared to its baseline. Moreover, DirPA yields noticeable gains on broader parent-level metrics (Table 6b), consistently outperforming the non-DirPA baselines, except when paired with FL in the 1-shot benchmark task. The greatest improvement is observed for 1-shot CE, where DirPA achieves 27% performance gain in accuracy and 20% in F1-score.

**Latvia** For Latvia (Table 7a), incorporating prior augmentation with FL yields substantial gains in kappa and accuracy across all few-shot tasks. Most notably, for 5-shot, DirPA improves all three metrics compared to the FL baseline,

showing increases of 41% (kappa), 44% (accuracy), and 9% (F1-score). Although the improvements are less consistent when paired with CE, the method still provides a performance boost in terms of kappa and accuracy for 1-, 10-, and 20-shot settings. Similar results are observed for HCAT level 3 in Table 7b, where FL DirPA is the top performer in nearly every scenario, with the sole exception of the F1-score at 100-shots. Meanwhile, adding prior augmentation to CE improves both accuracy and F1-scores on parent-level classes for 1-, 10-, and 20-shot settings.

**Lithuania** For fine-grained classification (Table 8a), incorporating DirPA yields considerable improvements in both Cohen’s kappa and accuracy across all few-shot scenarios and loss functions. When combined with FL, the method also enhances F1-scores across nearly all benchmarks, except for the 10-shot scenario, where it exhibits a loss of around 7%. For CE, this multi-metric improvement is observed for both 1- and 20-shot tasks. Regarding HCAT level 3 performance (Table 8b), DirPA consistently outperforms its baselines across both evaluation metrics and all few-shot settings, regardless of the loss function.

**Portugal** The results for Portugal (Table 9) are more nuanced. However, DirPA still facilitates several key improvements. For HCAT level 6, it achieves joint superiority across all three metrics for 10- and 20-shot when used with CE and for 10-, 20-, and even 100-shot when adding it to FL. Parent-level metrics also benefit substantially, particularly in the mid-range few-shot tasks ( $k \in \{5, 10, 20\}$ ) for CE and for  $k \in \{1, 10, 100\}$  for FL.

**Slovakia** For fine-grained classification in Slovakia (Table 10a), adding Dirichlet priors to CE leads to a marked improvement in kappa and accuracy for  $k \geq 5$ , with 5- and 10-shot tasks showing superiority across all three metrics. When paired with FL, DirPA outperforms the standard FL baseline for every few-shot scenario in terms of kappa and accuracy, while also achieving higher F1-scores for 5-, 10-, and 20-shot. On broader parent-level crop types (Table 10b), adding Dirichlet prior augmentation consistently achieves higher accuracies and F1-scores, except for CE in the 10-shot benchmark, where it matches its baseline.

**Slovenia** Adding prior augmentation consistently improves both Cohen’s kappa and accuracy for all few-shot scenarios, regardless of the loss function used (Table 11a). Furthermore, for  $k \in \{1, 5, 20\}$ , it either improves or matches (20-shot CE) the F1-scores. For the 10- and 100-shot scenario, DirPA falls slightly behind the baselines, showing a marginally lower F1-score of 5% or 12% when incorporated with CE and 8% or 10% when added to FL. This performance advantage is even more pronounced for parent-level classes (Table 11b), where DirPA consistently achieves higher accuracies and F1-scores across all few-shot tasks and loss functions.

**Spain** For few-shot classification in Spain (Table 12), incorporating prior augmentation with CE results in consistent—and

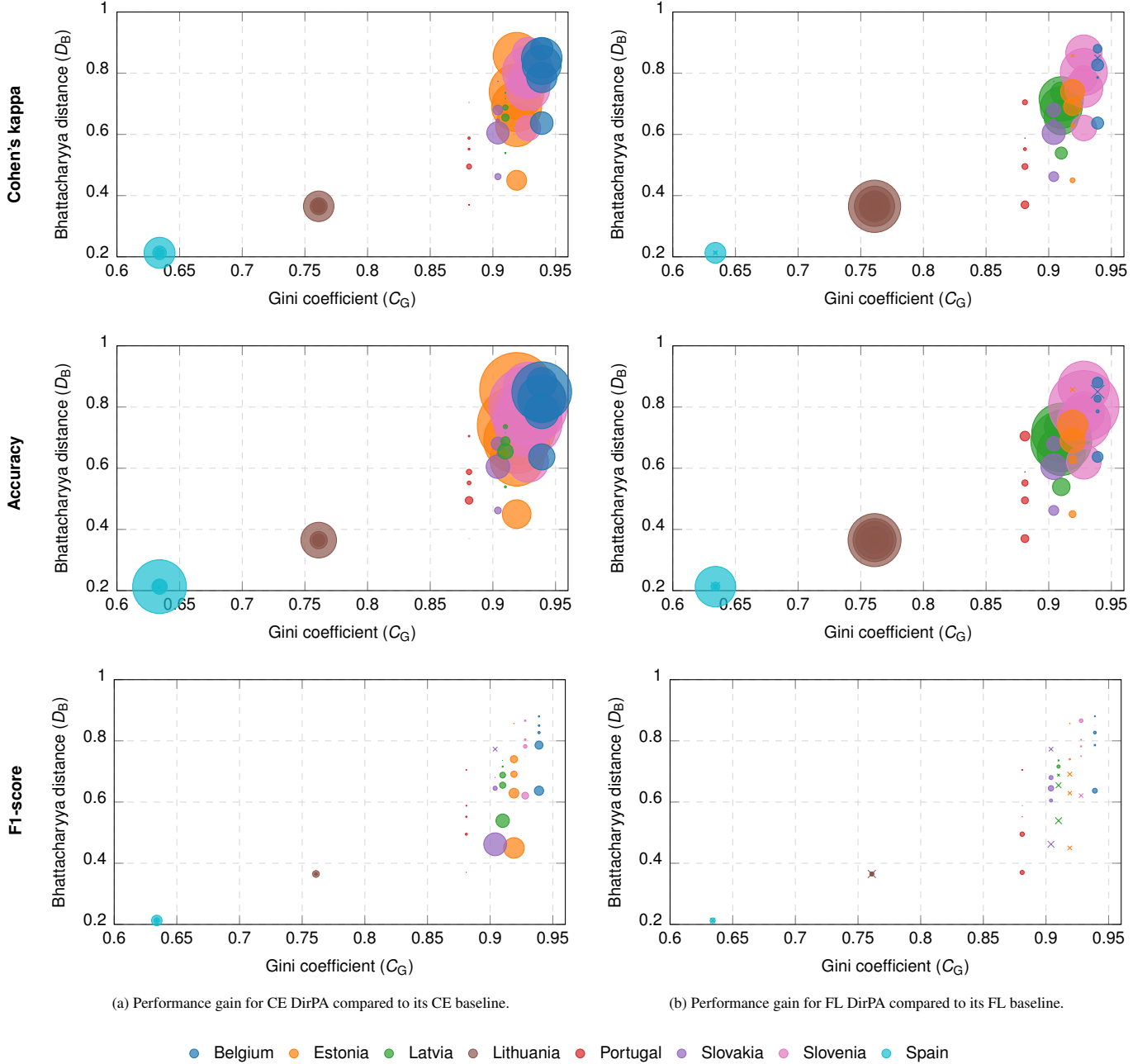


Figure 8. Performance gains achieved by applying DirPA, visualized relative to the Bhattacharyya distance (*cf.* Table 4) and Gini coefficient (*cf.* Table 3). Circular markers denote performance gains, while crosses represent losses of the DirPA method. The marker sizes indicate the magnitude of gains or losses compared to the respective baseline. An increasing  $D_B$  is equivalent to a decreasing number of  $k$  in the few-shot scenario and represents a bigger prior shift. For Lithuania and Spain,  $D_B$  stays constant since the relative class distribution remains the same in each few-shot task.

most often substantial—improvements across all metrics for both HCAT levels. In contrast, when paired with FL, DirPA shows less consistent gains, particularly regarding F1-scores. However, for 1-, 5-, and 20-shot, it substantially enhances both kappa and accuracy for HCAT level 6 (Table 12a). In the 20-shot scenario, DirPA demonstrates superiority over its FL baseline across all metrics. In contrast to other countries, the FL DirPA combination appears less effective for parent-level classes (Table 12b), where improvements are confined to the 1- and 20-shot benchmarks.

## 7. Discussion

The empirical results in Section 6 across eight diverse countries show a consistent and significant performance gain over standard baselines, particularly in low-shot regimes ( $k \leq 20$ ), as shown in Figures 8 and 9. This underscores the cross-dataset stability of the DirPA method, suggesting that the Dirichlet prior induces a form of universal regularization and improves model robustness. The chance-corrected gains in Cohen’s kappa across all countries confirm that these improvements represent a genu-

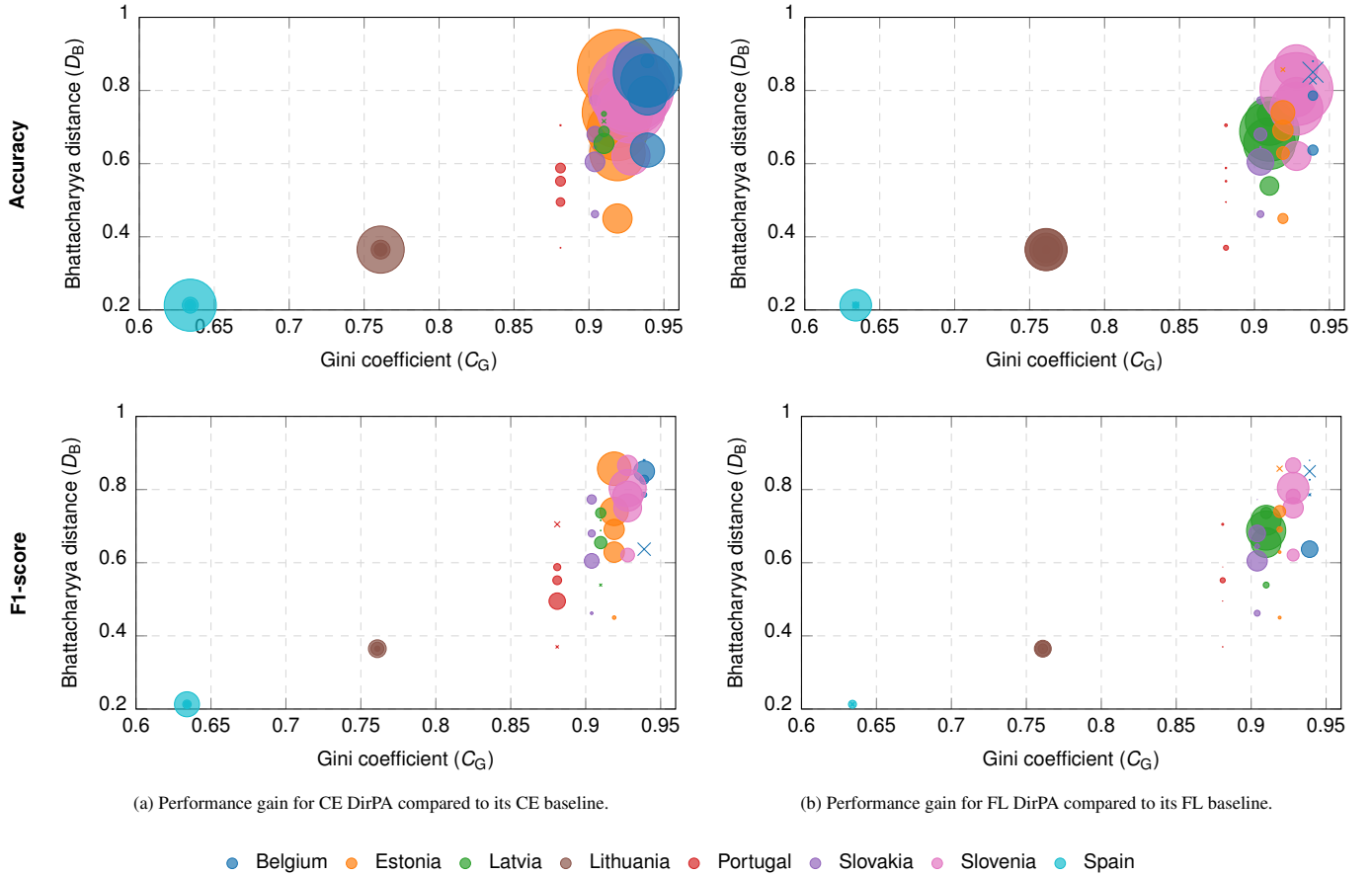


Figure 9. Performance gains on HCAT level 3 achieved by applying DirPA, visualized relative to the Bhattacharyya distance (cf. Table 4) and Gini coefficient (cf. Table 3). Circular markers denote performance gains, while crosses represent losses of the DirPA method. The marker sizes indicate the magnitude of gains or losses in metrics compared to the respective baseline. An increasing  $D_B$  is equivalent to a decreasing number of  $k$  in the few-shot scenario and represents a bigger prior shift. For Lithuania and Spain,  $D_B$  stays constant since the relative class distribution remains the same in each few-shot task.

ine increase in discriminative power, rather than being a result of frequentist exploitation.

In low-shot regimes, when training sets are inherently balanced by the  $k$ -shot sampling strategy, and data is extremely scarce, DirPA prevents feature hallucination. While standard Softmax forces a hard point-estimate choice, DirPA maps the features to a density on the  $(K - 1)$ -simplex, as visualized in Figure 10. This allows the model to capture uncertainty arising from data scarcity, preventing overconfidence in poor features and leading to higher kappa scores. As a result, DirPA maximizes system-wide reliability, achieving large gains in kappa and accuracy, cf. Figure 8. Conversely, in high-shot regimes, where the natural class imbalance begins to re-emerge in the training data (Table 4), the prior augmentation shifts to preventing majority-class dominance. Consequently, higher performance gains in class-specific metrics are observed for higher  $k$  (equivalent to lower  $D_B$ ), meaning bigger prior shifts. Importantly, integrating DirPA does not introduce performance penalties in higher-shot environments. Confirming our previous findings in Reuss et al. (2026a), all evaluated methods converge to a similar performance ceiling in high-shot scenarios. Ultimately, the efficacy of DirPA is strongly correlated with the dataset’s

structural inequality. Countries with extreme class imbalance (Table 3), like Belgium ( $C_G = 0.939$ ), Slovenia ( $C_G = 0.928$ ), and Estonia ( $C_G = 0.919$ ), benefit most from this regularization, where countries with smaller Gini coefficients, such as Spain and Lithuania, often benefit less in terms of kappa, as visualized in Figures 8 and 9.

While initial experiments (Reuss et al., 2026a) did not show any improvement in F1-scores, our results on the adapted, real-world dataset split, as outlined in Section 3.2, often demonstrate DirPA’s superiority even in terms of F1-scores. This indicates that for DirPA to effectively improve per-class discriminative power, the model must be exposed to training samples from all target classes. By ensuring representation of all classes in the training set and maximizing overlap between splits, the method can correctly regularize the feature space based on the actual crop types rather than generalizing to unseen categories. Nevertheless, most consistent improvements are observed in Cohen’s kappa and overall accuracy. As noted by Reuss et al. (2026b), this represents a necessary trade-off to achieve superior global performance. The strong regularization required for overall stability can sometimes lead to over-smoothed boundaries for high-resource categories. This minor localized loss is

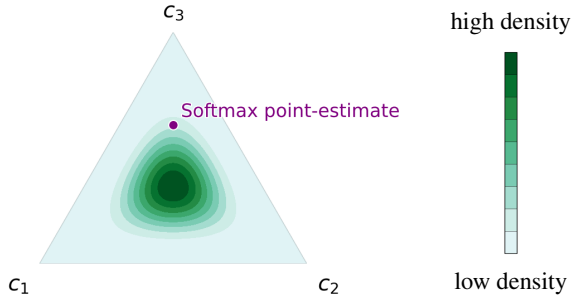


Figure 10. Comparison of predictive output space on the 2-simplex  $\Delta^2$  for a three-class classification ( $c_1, c_2, c_3$ ). The Softmax function reduces feature information to a single coordinate on the simplex, producing a point estimate. In contrast, the Dirichlet distribution maps features to a probability density over the simplex, thereby capturing epistemic uncertainty.

outweighed by the improved global classification reliability ( $\kappa$ ), ensuring the model is more effective at handling the dataset’s full class variability. Overall, F1-scores remain constrained by the dataset’s extreme class imbalance and high cardinality. These lower values reflect the fundamental difficulty of maintaining high precision and recall across a large number of low-resource, long-tail classes, in particular in low-shot regimes.

A key finding is the superior performance of DirPA across broader parent classes, particularly in F1-scores. This also underscores the improved system robustness achieved by incorporating Dirichlet priors. Even in cases where the model fails to distinguish between fine-grained crop types—leading to lower fine-grained F1-scores—, it almost consistently better identifies the parent land cover category. The higher kappa scores and overall accuracies at the fine-grained level, paired with superior parent-level F1-scores, suggest that the system’s errors are often restricted to closely related sub-classes within the same correct parent category, rather than being total classification failures. This indicates that DirPA in addition acts as a hierarchical stabilizer, not just a class-specific one. However, in contrast to the performance gains for fine-grained classification, when evaluated on HCAT level 3, DirPA most often exhibits the highest performance gains in F1 with an increasing number of shots. This disparity in F1-score gains across different hierarchical levels reveals that DirPA’s regularization mechanism adapts to data availability. In very low-shot scenarios, it mitigates catastrophic misclassifications between unrelated land-cover types. As  $k$  increases and class features become better defined, it transitions from providing structural stability to refining class boundaries. This enhances the separation between closely related crop types, thus leading to higher gains in fine-grained F1-scores.

### 7.1. Asymmetric priors

While the symmetric Dirichlet ( $\alpha = \alpha \cdot \mathbf{1}$ ) serves as our robust baseline, we also investigated an asymmetric variant (Reuss et al., 2026a). Our intuition was to amplify the signal for a selected focus class, which we randomly sample at each step  $s$  and assign a different value to its concentration parameter  $\alpha$ . However, empirical results on Estonia, Belgium, and Slovenia

showed that this asymmetric sampling did not yield a performance gain over the simpler symmetric version. This suggests that the original method already provides sufficient regularization and that the additional complexity of a class-specific focus does not offer further discriminative advantages.

## 8. Conclusion

This study presents a geographically extended application of the **Dirichlet Prior Augmentation** method, which aims to bridge the prior shift between balanced few-shot training sets and imbalanced test data. By augmenting the training data with dynamically sampled Dirichlet pseudo-priors, DirPA encourages the model to learn feature representations that are robust across a variety of potential class distributions. Instead of converging to a rigid point estimate based on a fixed prior, the model is regularized to maintain discriminative power across the  $(K - 1)$ -simplex, capturing the uncertainty inherent in few-shot regimes.

Our evaluation across eight EU countries demonstrates the method’s cross-dataset robustness, yielding consistent improvements in Cohen’s kappa and overall accuracy. In particular for low-shot regimes, DirPA maximizes system-wide reliability. Notably, the most substantial gains were observed in countries with extreme class imbalance (high Gini coefficients). This confirms that DirPA effectively mitigates the structural inequalities inherent in real-world few-shot crop classification datasets. Crucially, our experiments with a realistic, comprehensive dataset split demonstrate that DirPA’s ability to enhance F1-scores depends on the model being exposed to all target classes during training, rather than attempting to generalize to zero-shot categories (cf. Reuss et al., 2026a). Given the highest gains in higher-shot scenarios, we found that DirPA maximizes class-specific performance when there is enough data to learn class boundaries.

Furthermore, while the method occasionally trades off fine-grained class-specific performance due to the over-smoothing of decision boundaries, it notably enhances hierarchical consistency, ensuring that parent-level land cover classes are correctly identified even when sub-class distinctions fail. This superior performance provides a compelling argument for incorporating DirPA into hierarchical crop-type classification frameworks in future work.

Despite the effectiveness of the DirPA method, challenges remain. For instance, its performance gain is highly dependent on identifying the optimal values for hyperparameters  $\alpha$  and  $\tau$ , cf. Appendix B.2.1. Hence, additional preliminary experiments aimed at dynamically learning the Dirichlet concentration parameter  $\alpha$ . However, we were not yet able to achieve significant improvements over the fixed-parameter setup. These initial results suggest that optimizing  $\alpha$  is non-trivial and warrants further investigation.

### CRedit authorship contribution statement

**J. Reuss:** Conceptualization, Data curation, Formal analysis, Investigation, Methodology, Resources, Software, Validation,

Table A.13. Hardware specifications.

Node(s)	GPU	VRAM	CPU	vCPUs	Architecture
1-3	NVIDIA RTX A6000	48GB	Intel Xeon	12	Ampere
4	NVIDIA A100-SXM4	40GB	AMD EPYC	24	Ampere

Table B.14. Pre-training hyperparameters. The hyperparameters utilized during pre-training, along with their corresponding valid values.

hyperparameter	value / value range
training/tuning epochs	100
tuning trials per setup	24
tuning warmup steps (batches)	5000
early stopping patience (epochs)	15
batch size $b$	256
learning rate $\beta$	$[10^{-4}, 10^{-2}]$
cosine annealing cycles	1
cosine annealing cycles warmup epochs	1
label smoothing factor	0.1

Visualization, Writing – original draft, Writing – review & editing. **E. Gikalo:** Visualization, Writing – original draft, Writing – review & editing. **M. Körner:** Funding acquisition, Project administration, Supervision, Writing – review & editing.

## Acknowledgments

The project is funded by the German Federal Ministry for Economic Affairs and Energy based on a decision by the German Bundestag under the funding references 50EE2007B (J. Reuss, E. Gikalo, and M. Körner) and 50EE2105 (M. Körner).

## Appendix A. Implementation and hardware details

We implemented all algorithms within the PyTorch framework (Paszke et al., 2019) for machine learning and automatic differentiation. For all experiments, we used the *Adam* optimizer.

The experiments were distributed across four virtualized machines with different hardware specifications, as detailed in Table A.13.

## Appendix B. Hyperparameter tuning

### Appendix B.1. Pre-training

The performance on the validation set is used to select the best hyperparameters and the model to be used for fine-tuning. We employ a total of 5000 warm-up steps (corresponding to batches) and keep the top 75th percentile of runs. We use the best validation accuracy to determine the best pre-training epoch and model state, which is subsequently used to initialize the model backbone weights before fine-tuning. The exact hyperparameter values or value ranges are listed in Table B.14.

### Appendix B.2. Fine-tuning

For fine-tuning, we use only 300 warm-up steps while again keeping the 75th percentile of runs. Furthermore, we treat backbone freezing as a tunable hyperparameter. Finally, the model

Table B.15. General fine-tuning hyperparameters. The hyperparameters utilized during fine-tuning, along with their corresponding valid values.

hyperparameter	value / value range
training/tuning epochs	200
tuning trials per setup <sup>†</sup>	{32, 40, 72, 80}
tuning warmup steps (batches)	300
early stopping patience (epochs)	20
batch size $b$	16
head learning rate $\beta_{\text{head}}$	$[10^{-6}, 10^{-2}]$
backbone learning rate $\beta_{\text{backbone}}$	$[10^{-7}, 10^{-3}]$
backbone freezing (epochs)	{0, 2, 5, 8, 15}
focal loss focusing parameter $\gamma$	{1.0, 1.5, 2.0, 3.0}

<sup>†</sup> Depending on the algorithm and, hence, tunable parameters, we use a different number of tuning trials. We set them as follows: 32 (CE), 40 (FL), 72 (CE with DirPA), 80 (FL with DirPA).

Table B.16. DirPA fine-tuning hyperparameters. The DirPA hyperparameters utilized during fine-tuning, along with their corresponding valid values.

hyperparameter	value / value range
DirPA concentration $\alpha$	{0.01, 0.1, 0.5, 1.0, 2.0, 3.0, 5.0}
DirPA scaling factor $\tau$	{0.5, 1.0, 2.0, 5.0, 10.0}

state exhibiting the best validation kappa score is used to compute the final reported model performance metrics on the fine-tuning test dataset. The exact hyperparameter values or value ranges are listed in Tables B.15 and B.16.

### Appendix B.2.1. DirPA hyperparameters analysis

Tables B.17 and B.18 show the median values of the DirPA hyperparameters  $\alpha$  and  $\tau$  selected for the final training runs across countries and few-shot scenarios. Although a comparison of these values does not reveal a consistent numerical pattern or trend, optimal values for  $\alpha$  are rather low, while for  $\tau$ , 10 was most often selected, resulting in a strong prior adjustment. Furthermore, an analysis of DirPA hyperparameter importances across all investigated countries and loss functions does not provide a clear trend. In fact, Tables B.19 and B.20 show that the relative importance of  $\alpha$  and  $\tau$  varies severely across countries and data regimes. Thus, as optimal settings depend heavily on the specific dataset, we conclude that there is no universal recommendation for configuring these hyperparameters. We therefore recommend using a predefined search space of possible values, as detailed in Table B.16, and tuning to find the optimal value.

### Appendix B.2.2. Runtime analysis

Tables B.21 to B.28 show a comparison of runtimes with and without the DirPA method. While these values are not strictly comparable, as the experiments were partially conducted in parallel on multiple machines with varying hardware specifications (cf. Table A.13), they still give an indication of the training time required. Furthermore, the training time is influenced by early stopping. This may also result in greater standard deviations. Nevertheless, no clear trend suggests that applying Dirichlet priors substantially increases training time. In fact, DirPA often requires less training time on average than its counterpart.

Table B.17. Median of selected optimal values of DirPA hyperparameters with cross-entropy loss, calculated based on finding the optimal hyperparameter values to maximize Cohen’s kappa. The median is calculated over five Optuna studies with different random seeds.

(a) Concentration parameter $\alpha$ .					
Country	benchmark task ( $k$ -shot)				
	1	5	10	20	100
Belgium	0.10	1.00	2.00	0.10	0.50
Estonia	0.50	0.10	0.10	0.01	1.00
Latvia	0.50	1.00	0.50	3.00	0.75
Lithuania	0.75	1.00	1.00	0.75	3.00
Portugal	1.00	0.75	0.75	1.00	1.50
Slovakia	5.00	0.75	0.50	0.75	1.00
Slovenia	2.00	2.00	0.10	0.10	1.00
Spain	0.10	3.00	0.50	2.00	3.00

(b) Temperature parameter $\tau$ .					
Country	benchmark task ( $k$ -shot)				
	1	5	10	20	100
Belgium	2.0	5.0	5.0	10.0	5.0
Estonia	5.0	10.0	5.0	5.0	10.0
Latvia	5.0	10.0	10.0	5.0	2.0
Lithuania	10.0	5.0	5.0	2.0	5.0
Portugal	2.0	5.0	2.0	1.0	1.0
Slovakia	10.0	10.0	5.0	10.0	10.0
Slovenia	10.0	10.0	10.0	10.0	10.0
Spain	10.0	2.0	2.0	5.0	5.0

Table B.18. Median of selected optimal values of DirPA hyperparameters with focal loss, calculated based on finding the optimal hyperparameter values to maximize Cohen’s kappa. The median is calculated over five Optuna studies with different random seeds.

(a) Concentration parameter $\alpha$ .					
Country	benchmark task ( $k$ -shot)				
	1	5	10	20	100
Belgium	2.00	0.10	0.50	2.00	0.50
Estonia	0.10	0.10	0.01	0.10	0.10
Latvia	1.00	0.75	0.01	1.50	1.00
Lithuania	2.00	0.10	0.01	0.10	0.50
Portugal	0.50	1.00	0.50	0.50	3.00
Slovakia	3.00	0.75	0.75	1.50	1.00
Slovenia	0.10	0.01	1.50	0.10	0.10
Spain	0.50	1.00	0.50	0.50	0.50

(b) Temperature parameter $\tau$ .					
Country	benchmark task ( $k$ -shot)				
	1	5	10	20	100
Belgium	10.0	10.0	10.0	10.0	1.000
Estonia	10.0	2.0	5.0	10.0	5.0
Latvia	10.0	1.0	5.0	5.0	2.0
Lithuania	10.0	5.0	1.0	10.0	2.0
Portugal	10.0	5.0	1.0	2.0	2.0
Slovakia	5.0	10.0	10.0	10.0	10.0
Slovenia	2.0	10.0	10.0	5.0	10.0
Spain	5.0	10.0	1.0	1.0	2.0

Table B.19. Relative importance of DirPA hyperparameters with cross-entropy loss, calculated based on finding the optimal hyperparameter values to maximize Cohen’s kappa. The values represent the median over five Optuna studies with different random seeds. The relative importance is calculated based on a total of five tunable hyperparameters.

(a) Concentration parameter $\alpha$ .					
Country	benchmark task ( $k$ -shot)				
	1	5	10	20	100
Belgium	0.139	0.341	0.189	0.230	0.332
Estonia	0.273	0.426	0.437	0.589	0.163
Latvia	0.121	0.146	0.171	0.205	0.106
Lithuania	0.086	0.135	0.086	0.069	0.058
Portugal	0.111	0.140	0.200	0.147	0.086
Slovakia	0.070	0.144	0.090	0.179	0.112
Slovenia	0.290	0.376	0.242	0.351	0.120
Spain	0.250	0.205	0.090	0.165	0.191

(b) Temperature parameter $\tau$ .					
Country	benchmark task ( $k$ -shot)				
	1	5	10	20	100
Belgium	0.111	0.113	0.091	0.410	0.104
Estonia	0.057	0.325	0.165	0.123	0.413
Latvia	0.148	0.109	0.220	0.194	0.118
Lithuania	0.156	0.226	0.130	0.137	0.141
Portugal	0.110	0.312	0.079	0.142	0.075
Slovakia	0.040	0.298	0.251	0.249	0.224
Slovenia	0.062	0.193	0.144	0.273	0.369
Spain	0.078	0.054	0.041	0.089	0.108

Table B.20. Relative importance of DirPA hyperparameters with focal loss, calculated based on finding the optimal hyperparameter values to maximize Cohen’s kappa. The values represent the median over five Optuna studies with different random seeds. Please note that an additional hyperparameter (FL focus parameter  $\gamma$ ) was taken into account in these studies. Thus, the relative importance of  $\alpha$  and  $\tau$  is calculated against a broader set of parameters (six in total) and, therefore, not directly comparable to the ones in Table B.19.

(a) Concentration parameter $\alpha$ .					
Country	benchmark task ( $k$ -shot)				
	1	5	10	20	100
Belgium	0.114	0.209	0.130	0.344	0.228
Estonia	0.560	0.319	0.373	0.258	0.121
Latvia	0.161	0.245	0.213	0.240	0.390
Lithuania	0.082	0.284	0.472	0.415	0.219
Portugal	0.234	0.106	0.229	0.176	0.312
Slovakia	0.046	0.141	0.111	0.094	0.084
Slovenia	0.236	0.360	0.277	0.566	0.383
Spain	0.341	0.237	0.200	0.168	0.237

(b) Temperature parameter $\tau$ .					
Country	benchmark task ( $k$ -shot)				
	1	5	10	20	100
Belgium	0.146	0.254	0.083	0.178	0.171
Estonia	0.103	0.157	0.119	0.213	0.022
Latvia	0.131	0.243	0.163	0.113	0.095
Lithuania	0.115	0.176	0.093	0.057	0.107
Portugal	0.107	0.126	0.048	0.134	0.123
Slovakia	0.118	0.207	0.132	0.398	0.334
Slovenia	0.071	0.136	0.081	0.118	0.173
Spain	0.118	0.034	0.056	0.076	0.059

Table B.21. Fine-tuning runtimes for final training on **Belgium**. We present the average training time (in minutes) as mean  $\pm$  standard deviation over five runs (seeds). The fastest run time per few-shot scenario is marked in **bold**.

algorithm/loss	benchmark task ( $k$ -shot)				
	1	5	10	20	100
CE	13.3 $\pm$ 8.4	11.5 $\pm$ 4.4	13.6 $\pm$ 3.1	12.3 $\pm$ 2.5	20.0 $\pm$ 3.6
CE DirPA	9.62 $\pm$ 0.58	10.4 $\pm$ 1.4	10.12 $\pm$ 0.99	12.6 $\pm$ 2.9	17.5 $\pm$ 1.7
FL	6.7 $\pm$ 2.3	<b>6.9 <math>\pm</math> 2.7</b>	10.8 $\pm$ 4.1	10.6 $\pm$ 2.9	13.4 $\pm$ 5.1
FL DirPA	<b>6.7 <math>\pm</math> 1.5</b>	7.1 $\pm$ 3.1	<b>9.5 <math>\pm</math> 1.6</b>	<b>8.7 <math>\pm</math> 1.5</b>	<b>12.7 <math>\pm</math> 1.7</b>

Table B.22. Fine-tuning runtimes for final training on **Estonia**. We present the average training time (in minutes) as mean  $\pm$  standard deviation over five runs (seeds). The fastest run time per few-shot scenario is marked in **bold**.

algorithm/loss	benchmark task ( $k$ -shot)				
	1	5	10	20	100
CE	15 $\pm$ 13	7.35 $\pm$ 0.80	8.9 $\pm$ 1.6	9.9 $\pm$ 1.6	17.2 $\pm$ 5.6
CE DirPA	<b>9.1 <math>\pm</math> 2.6</b>	<b>7.0 <math>\pm</math> 1.1</b>	<b>8.5 <math>\pm</math> 1.8</b>	<b>8.6 <math>\pm</math> 1.2</b>	<b>12.4 <math>\pm</math> 2.4</b>
FL	9.1 $\pm$ 2.7	48 $\pm$ 36	37 $\pm$ 36	54 $\pm$ 35	32 $\pm$ 30
FL DirPA	51 $\pm$ 32	52 $\pm$ 57	37 $\pm$ 35	21 $\pm$ 31	19.4 $\pm$ 9.0

Table B.23. Fine-tuning runtimes for final training on **Lithuania**. We present the average training time (in minutes) as mean  $\pm$  standard deviation over five runs (seeds). The fastest run time per few-shot scenario is marked in **bold**.

algorithm/loss	benchmark task ( $k$ -shot)				
	1	5	10	20	100
CE	<b>8.0 <math>\pm</math> 2.7</b>	11.5 $\pm$ 6.4	<b>8.8 <math>\pm</math> 2.0</b>	<b>7.7 <math>\pm</math> 3.5</b>	10.4 $\pm$ 1.7
CE DirPA	15.5 $\pm$ 3.2	12.2 $\pm$ 3.4	13.18 $\pm$ 0.19	11.1 $\pm$ 2.4	<b>10.2 <math>\pm</math> 5.4</b>
FL	14.1 $\pm$ 4.7	11.5 $\pm$ 3.1	12.5 $\pm$ 4.2	13.0 $\pm$ 3.5	11.5 $\pm$ 2.9
FL DirPA	12.8 $\pm$ 3.1	<b>11.4 <math>\pm</math> 2.5</b>	9.6 $\pm$ 2.4	12.3 $\pm$ 1.7	11.86 $\pm$ 0.88

Table B.24. Fine-tuning runtimes for final training on **Latvia**. We present the average training time (in minutes) as mean  $\pm$  standard deviation over five runs (seeds). The fastest run time per few-shot scenario is marked in **bold**.

algorithm/loss	benchmark task ( $k$ -shot)				
	1	5	10	20	100
CE	9.3 $\pm$ 1.9	12.2 $\pm$ 5.2	11.1 $\pm$ 1.2	13.0 $\pm$ 2.4	19.4 $\pm$ 6.5
CE DirPA	9.9 $\pm$ 1.1	10.4 $\pm$ 2.2	<b>8.5 <math>\pm</math> 2.7</b>	10.8 $\pm$ 3.0	<b>13.7 <math>\pm</math> 5.1</b>
FL	9.11 $\pm$ 0.73	9.0 $\pm$ 1.1	9.30 $\pm$ 0.30	11.5 $\pm$ 4.6	17.7 $\pm$ 3.6
FL DirPA	<b>9.0 <math>\pm</math> 1.4</b>	<b>8.67 <math>\pm</math> 0.92</b>	11.1 $\pm$ 1.6	<b>9.9 <math>\pm</math> 2.5</b>	15.6 $\pm$ 1.2

Table B.25. Fine-tuning runtimes for final training on **Portugal**. We present the average training time (in minutes) as mean  $\pm$  standard deviation over five runs (seeds). The fastest run time per few-shot scenario is marked in **bold**.

algorithm/loss	benchmark task ( $k$ -shot)				
	1	5	10	20	100
CE	6.1 $\pm$ 2.3	<b>7.1 <math>\pm</math> 1.3</b>	7.6 $\pm$ 2.1	<b>7.1 <math>\pm</math> 2.2</b>	11.3 $\pm$ 6.1
CE DirPA	<b>5.0 <math>\pm</math> 3.0</b>	7.4 $\pm$ 2.6	<b>6.3 <math>\pm</math> 2.1</b>	7.5 $\pm$ 1.9	<b>9.9 <math>\pm</math> 4.5</b>
FL	21 $\pm$ 28	28 $\pm$ 30	36 $\pm$ 38	49 $\pm$ 59	14.7 $\pm$ 5.5
FL DirPA	7.0 $\pm$ 3.5	21 $\pm$ 32	23 $\pm$ 26	34 $\pm$ 40	12.9 $\pm$ 8.2

Table B.26. Fine-tuning runtimes for final training on **Slovakia**. We present the average training time (in minutes) as mean  $\pm$  standard deviation over five runs (seeds). The fastest run time per few-shot scenario is marked in **bold**.

algorithm/loss	benchmark task ( $k$ -shot)				
	1	5	10	20	100
CE	7.89 $\pm$ 0.82	10.0 $\pm$ 3.6	9.7 $\pm$ 1.7	11.0 $\pm$ 2.9	16.1 $\pm$ 5.8
CE DirPA	7.2 $\pm$ 1.4	<b>7.1 <math>\pm</math> 3.3</b>	<b>8.0 <math>\pm</math> 2.0</b>	<b>7.6 <math>\pm</math> 2.5</b>	14.1 $\pm$ 3.7
FL	9.4 $\pm$ 2.5	11.3 $\pm$ 2.6	12.1 $\pm$ 6.1	12.7 $\pm$ 2.7	22 $\pm$ 16
FL DirPA	<b>6.6 <math>\pm</math> 2.6</b>	8.8 $\pm$ 4.0	9.5 $\pm$ 3.4	11.4 $\pm$ 1.4	<b>12.2 <math>\pm</math> 2.3</b>

Table B.27. Fine-tuning runtimes for final training on **Slovenia**. We present the average training time (in minutes) as mean  $\pm$  standard deviation over five runs (seeds). The fastest run time per few-shot scenario is marked in **bold**.

algorithm/loss	benchmark task ( $k$ -shot)				
	1	5	10	20	100
CE	<b>6.8 <math>\pm</math> 2.2</b>	<b>9.55 <math>\pm</math> 0.94</b>	<b>11.4 <math>\pm</math> 4.2</b>	<b>10.6 <math>\pm</math> 5.6</b>	21.1 $\pm$ 6.2
CE DirPA	12.5 $\pm$ 2.0	12.1 $\pm$ 1.2	11.5 $\pm$ 1.1	11.9 $\pm$ 4.8	<b>14.3 <math>\pm</math> 4.4</b>
FL	8.6 $\pm$ 4.1	10.5 $\pm$ 2.0	11.7 $\pm$ 2.9	14.9 $\pm$ 8.5	19.4 $\pm$ 9.1
FL DirPA	10.2 $\pm$ 2.3	12.3 $\pm$ 3.9	13.3 $\pm$ 2.7	13.0 $\pm$ 1.4	17.3 $\pm$ 3.3

Table B.28. Fine-tuning runtimes for final training on **Spain**. We present the average training time (in minutes) as mean  $\pm$  standard deviation over five runs (seeds). The fastest run time per few-shot scenario is marked in **bold**.

algorithm/loss	benchmark task ( $k$ -shot)				
	1	5	10	20	100
CE	<b>6.56 <math>\pm</math> 0.84</b>	<b>6.42 <math>\pm</math> 0.59</b>	7.2 $\pm$ 1.3	6.7 $\pm$ 1.4	8.3 $\pm$ 3.1
CE DirPA	16.0 $\pm$ 6.1	31 $\pm$ 28	42 $\pm$ 38	39 $\pm$ 32	52 $\pm$ 31
FL	8.4 $\pm$ 2.6	8.2 $\pm$ 2.3	<b>6.6 <math>\pm</math> 2.2</b>	<b>7.2 <math>\pm</math> 1.7</b>	<b>7.1 <math>\pm</math> 1.9</b>
FL DirPA	10.2 $\pm$ 3.6	10.8 $\pm$ 3.9	11.4 $\pm$ 5.3	9.2 $\pm$ 4.3	10.1 $\pm$ 4.4

## References

- Akiba, T., Sano, S., Yanase, T., Ohta, T., Koyama, M., 2019. Optuna: A next-generation hyperparameter optimization framework, in: ACM SIGKDD International Conference on Knowledge Discovery and Data Mining (KDD), pp. 2623–2631. doi:10.1145/3292500.3330701.
- Alem, A., Kumar, S., 2022. Transfer learning models for land cover and land use classification in remote sensing image. Applied Artificial Intelligence 36. doi:10.1080/08839514.2021.2014192.
- Bermúdez, J.D., Achancarray, P., Sanches, I., Cue La Rosa, L., Happ, P., Feitosa, R., 2017. Evaluation of recurrent neural networks for crop recognition from multitemporal remote sensing images, in: XXVII Congresso Brasileiro de Cartografia e XXVI Exposita, pp. 800–804.
- Bhattacharyya, A., 1946. On a measure of divergence between two multinomial populations. Sankhyā: The Indian Journal of Statistics (1933-1960) 7, 401–406.
- Ceriani, L., Verme, P., 2011. The origins of the gini index: Extracts from variabilità e mutabilità (1912) by corrado gini. The Journal of Economic Inequality 10, 421–443. doi:10.1007/s10888-011-9188-x.
- Daumé III, H., Marcu, D., 2005. A bayesian model for supervised clustering with the dirichlet process prior. Journal of Machine Learning Research 6, 1551–1577.
- Enache, S., Louis, J., Pflug, B., de Los Reyes, R., Lafrance, B., Clerc, S., Barrot, G., Alhammoud, B., Poustomis, F., Iannone, R.Q., Bruniquel, J., Boccia, V., Gascon, F., 2023. Copernicus sentinel-2 collection-1: A consistent dataset of multi-spectral imagery with enhanced quality, in: Proceedings of the IEEE International Geoscience and Remote Sensing Symposium (IGARSS), pp. 4302–4305. doi:10.1109/IGARSS52108.2023.10282362.

- European Environment Agency (EEA), 2016. Biogeographical regions. URL: <https://sdi.eea.europa.eu/catalogue/srv/api/records/11db8d14-f167-4cd5-9205-95638dfd9618>. visited on Dec. 29, 2025.
- European Space Agency (ESA), 2021. Copernicus sentinel-2 msi level-1c toa reflectance product. collection 1. doi:[10.5270/S2\\_-7421kth](https://doi.org/10.5270/S2_-7421kth).
- Finn, C., Abbeel, P., Levine, S., 2017. Model-agnostic meta-learning for fast adaptation of deep networks, in: International Conference on Machine Learning (ICML), pp. 1126–1135.
- Keraani, M.K., Mansour, K., Khlaifia, B., Chehata, N., 2022. Few shot crop mapping using transformers and transfer learning with sentinel-2 time series: Case of kairouan tunisia. The International Archives of the Photogrammetry, Remote Sensing and Spatial Information Sciences XLIII-B3-2022, 899–906. doi:[10.5194/isprs-archives-XLIII-B3-2022-899-2022](https://doi.org/10.5194/isprs-archives-XLIII-B3-2022-899-2022).
- Kluger, D.M., Wang, S., Lobell, D.B., 2021. Two shifts for crop mapping: Leveraging aggregate crop statistics to improve satellite-based maps in new regions. Remote Sensing of Environment 262. doi:[10.1016/j.rse.2021.112488](https://doi.org/10.1016/j.rse.2021.112488).
- Kurian, V., Jacob, V., Kuruvilla, J., 2024. Approach of transfer learning in remote sensing image classification, in: International Conference on Trends in Engineering Systems and Technologies (ICTEST), pp. 1–3. doi:[10.1109/ICTEST60614.2024.10576178](https://doi.org/10.1109/ICTEST60614.2024.10576178).
- Lin, T.Y., Goyal, P., Girshick, R., He, K., Dollár, P., 2020. Focal loss for dense object detection. IEEE Transactions on Pattern Analysis and Machine Intelligence 42, 318–327. doi:[10.1109/TPAMI.2018.2858826](https://doi.org/10.1109/TPAMI.2018.2858826).
- Lipton, Z., Wang, Y.X., Smola, A., 2018. Detecting and correcting for label shift with black box predictors, in: International Conference on Machine Learning (ICML), pp. 3122–3130.
- Louis, J., Devignot, O., Pessiot, L., 2022. Sentinel-2 MSI level-2A algorithms, products, and performance: Algorithm theoretical basis document. Technical Report S2-PDGS-MPC-ATBD-L2A, Issue 2.10. European Space Agency. URL: <https://step.esa.int/thirdparties/sen2cor/2.10.0/docs/S2-PDGS-MPC-L2A-ATBD-V2.10.0.pdf>. visited on Jan. 22, 2026.
- Mohammadi, S., Belgiu, M., Stein, A., 2024. Few-shot learning for crop mapping from satellite image time series. Remote Sensing 16. doi:[10.3390/rs16061026](https://doi.org/10.3390/rs16061026).
- Ochal, M., Patacchiola, M., Vazquez, J., Storkey, A., Wang, S., 2023. Few-shot learning with class imbalance. IEEE Transactions on Artificial Intelligence 4, 1348–1358. doi:[10.1109/TAI.2023.3298303](https://doi.org/10.1109/TAI.2023.3298303).
- Paszke, A., Gross, S., Massa, F., Lerer, A., Bradbury, J., Chanan, G., Killeen, T., Lin, Z., Gimelshein, N., Antiga, L., Desmaison, A., Kopf, A., Yang, E., DeVito, Z., Raison, M., Tejani, A., Chilamkurthy, S., Steiner, B., Fang, L., Bai, J., Chintala, S., 2019. PyTorch: An imperative style, high-performance deep learning library, in: Advances in Neural Information Processing Systems (NeurIPS).
- Rademacher, P., Doroslovački, M., 2021. Bayesian learning for regression using dirichlet prior distributions of varying localization, in: IEEE Statistical Signal Processing Workshop (SSP), pp. 236–240. doi:[10.1109/SSP49050.2021.9513745](https://doi.org/10.1109/SSP49050.2021.9513745).
- Reuss, J., Gikalo, E., Körner, M., 2026a. Mind the gap: Bridging prior shift in realistic few-shot crop-type classification. ISPRS Annals of the Photogrammetry, Remote Sensing and Spatial Information Sciences [arXiv:2511.16218](https://arxiv.org/abs/2511.16218). forthcoming.
- Reuss, J., Macdonald, J., Becker, S., Gikalo, E., Schultka, K., Richter, L., Körner, M., 2026b. Benchmarking for practice: Few-shot time-series crop-type classification on the EuroCropsML dataset. ISPRS Open Journal of Photogrammetry and Remote Sensing 19. doi:[10.1016/j.ophoto.2026.100117](https://doi.org/10.1016/j.ophoto.2026.100117).
- Reuss, J., Macdonald, J., Becker, S., Richter, L., Körner, M., 2025. The EuroCropsML time series benchmark dataset for few-shot crop type classification in Europe. Scientific Data 12. doi:[10.1038/s41597-025-04952-7](https://doi.org/10.1038/s41597-025-04952-7).
- Rouba, M., Larabi, M.E.A., 2023. Improving remote sensing classification with transfer learning: Exploring the impact of heterogenous transfer learning. Engineering Proceedings 56. doi:[10.3390/ASEC2023-15505](https://doi.org/10.3390/ASEC2023-15505).
- Rußwurm, M., Körner, M., 2020. Self-attention for raw optical satellite time series classification. ISPRS Journal of Photogrammetry and Remote Sensing 169, 421–435. doi:[10.1016/j.isprsjprs.2020.06.006](https://doi.org/10.1016/j.isprsjprs.2020.06.006).
- Rußwurm, M., Wang, S., Körner, M., Lobell, D., 2020. Meta-learning for few-shot land cover classification, in: Proceedings of the IEEE/CVF Conference on Computer Vision and Pattern Recognition Workshops (CVPRW), pp. 788–796. doi:[10.1109/cvprw50498.2020.00108](https://doi.org/10.1109/cvprw50498.2020.00108).
- Saini, R., Ghosh, S.K., 2018. Crop classification on single date sentinel-2 imagery using random forest and support vector machine. The International Archives of the Photogrammetry, Remote Sensing and Spatial Information Sciences XLII-5, 683–688. doi:[10.5194/isprs-archives-XLII-5-683-2018](https://doi.org/10.5194/isprs-archives-XLII-5-683-2018).
- Sainte Fare Garnot, V., Landrieu, L., Giordano, S., Chehata, N., 2020. Satellite image time series classification with pixel-set encoders and temporal self-attention, in: Proceedings of the IEEE/CVF Conference on Computer Vision and Pattern Recognition (CVPR), pp. 12322–12331. doi:[10.1109/CVPR42600.2020.01234](https://doi.org/10.1109/CVPR42600.2020.01234).

- Schneider, M., Broszeit, A., Körner, M., 2021. EuroCrops: A pan-european dataset for time series crop type classification, in: Conference on Big Data from Space (BiDS), Publications Office of the European Union. doi:[10.2760/125905](https://doi.org/10.2760/125905).
- Schneider, M., Schelte, T., Schmitz, F., Körner, M., 2023. Euro-crops: The largest harmonized open crop dataset across the european union. Scientific Data 10. doi:[10.1038/s41597-023-02517-0](https://doi.org/10.1038/s41597-023-02517-0).
- Sipka, T., Sulc, M., Matas, J., 2022. The hitchhiker’s guide to prior-shift adaptation, in: IEEE/CVF Winter Conference on Applications of Computer Vision (WACV), pp. 2031–2039. doi:[10.1109/WACV51458.2022.00209](https://doi.org/10.1109/WACV51458.2022.00209).
- Tseng, G., Kerner, H., Rolnick, D., 2022. Timl: Task-informed meta-learning for agriculture. [arXiv:2202.02124](https://arxiv.org/abs/2202.02124).
- Vaswani, A., Shazeer, N., Parmar, N., Uszkoreit, J., Jones, L., Gomez, A.N., Kaiser, Ł., Polosukhin, I., 2017. Attention is all you need, in: Advances in Neural Information Processing Systems (NeurIPS).
- Veilleux, O., Boudiaf, M., Piantanida, P., Ben Ayed, I., 2021. Realistic evaluation of transductive few-shot learning, in: Advances in Neural Information Processing Systems (NeurIPS), pp. 9290–9302.
- Wang, A.X., Tran, C., Desai, N., Lobell, D., Ermon, S., 2018. Deep transfer learning for crop yield prediction with remote sensing data, in: Proceedings of the ACM Conference on Computing and Sustainable Societies, pp. 1–5. doi:[10.1145/3209811.3212707](https://doi.org/10.1145/3209811.3212707).
- Wang, S., Rußwurm, M., Körner, M., Lobell, D.B., 2020. Meta-learning for few-shot time series classification, in: Proceedings of the IEEE International Geoscience and Remote Sensing Symposium (IGARSS), pp. 7041–7044. doi:[10.1109/IGARSS39084.2020.9441016](https://doi.org/10.1109/IGARSS39084.2020.9441016).